# Plasma Chemistry and Kinetics in Low Pressure Oxygen Discharges: The significance of metastable states

Jón Tómas Guðmundsson[1,2]

[1] Science Institute, University of Iceland, Reykjavik, Iceland
[2]Department of Space and Plasma Physics,
School of Electrical Engineering and Computer Science,
KTH Royal Institute of Technology, SE-100 44, Stockholm, Sweden
tumi@hi.is

22th International School on
Low Temperature Plasma Physics: Basics and Applications,
Physikzentrum Bad Honnef, Germany

# *Outline*

- The oxygen discharge is of significance in various materials processing applications including
  - etching of polymer films
  - ashing of photoresist
  - oxidation
- The oxygen chemistry is complicated due to the presence of metastable atomic and molecular species
- It is in particular the two low lying metastable molecular states designated by $a^1\Delta_g$ and $b^1\Sigma_g^+$, which are located 0.98 and 1.627 eV above the ground state, respectively
- It is well established that collisions with these metastable states have in many cases larger cross sections and thus higher reaction rates than corresponding collisions with the ground state molecule
- The discharge electronegativity is dictated by these metastable states

# *Outline*

- A. Global (volume averaged) chemistry models
  - A1 The oxygen discharge
    - chlorine dilution
- B. 1D particle-in-cell/Monte Carlo collision simulation
  - B.1 Capacitively Coupled Oxygen Discharge at 13.56 MHz
    - pressure dependence
    - driving frequency dependence
    - surface quenching of $O_2(a^1\Delta_g)$
    - the effect of $\gamma_{\mathrm{see}}(\mathcal{E})$
- C. Summary

# A. Global (volume averaged) chemistry models

# *Global (volume averaged) chemistry models*

- The main idea of a global model is to generate a model that encompasses a large number of reactions in order to model a processing plasma with a limited computing power by neglecting the complexity which arises when spatial variations are considered
- Thus the model does not describe spatial distribution but captures scalings of plasma parameters with control parameters
- The model allows us to investigate various phenomena, such as the effects of excited species, negative ions and particular reactions on the overall discharge

# *Global (volume averaged) chemistry models*

- The densities of all species are assumed to be volume averaged
- For an electropositive discharge the positive-ion densities are assumed to have a uniform profile throughout the discharge except near the wall, where the density is assumed to drop sharply to a sheath-edge density $n_{\mathrm{IS}}$
- The electron energy distribution function (EEDF) is assumed (usually Maxwellian)
- The ion and neutral temperature have to be assumed

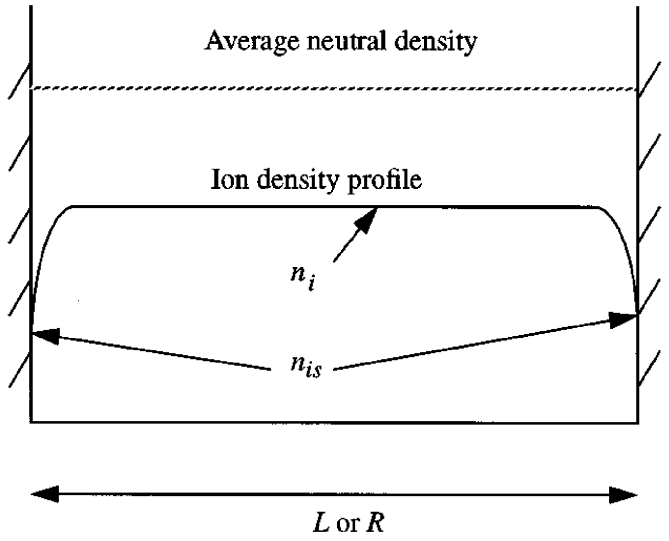


Lee and Lieberman *JVSTA*, **13** (1995) 368

# *Global (volume averaged) chemistry models*

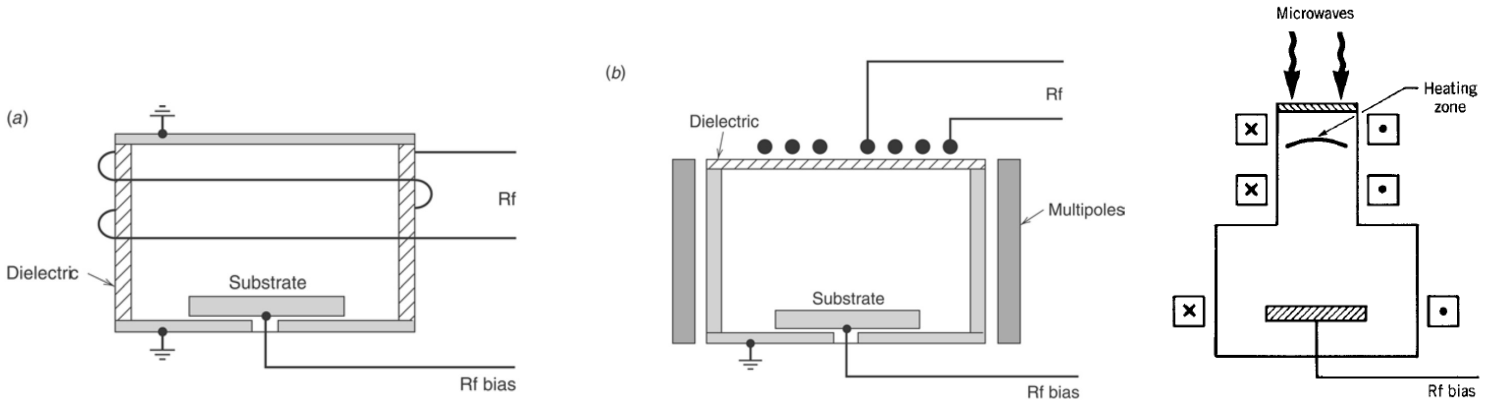


From Lieberman and Lichtenberg (2005)

- This kind of model can be applied to explore the plasma chemistry of low pressure high density discharges such as
  - inductively coupled discharge
  - electron cyclotron resonance (ECR) discharge

# A.1 Global (volume averaged) chemistry models – oxygen

# *The global (volume averaged) model*

- A steady state global (volume averaged) model was developed for the oxygen discharge
- The following species are included
  - electrons
  - the ground state oxygen molecule $O_2(X\,^3\Sigma_g^-, v = 0)$,
  - The metastable oxygen molecules $O_2(a^1\Delta_g)$, $O_2(b^1\Sigma_g^+)$ and the metastable Herzberg states $O_2(A^3\Sigma_u^+, A'^3\Delta_u, c^1\Sigma_u^-)$
  - the ground state oxygen atom $O(^3P)$
  - the metastable oxygen atom $O(^1D)$
  - the negative oxygen ions $O^-$ and $O_2^-$
  - the positive oxygen ions $O^+$ and $O_2^+$
  - Ozone $O_3$ and its ions $O_3^+$ and $O_3^-$
- The content of the chamber is assumed to be nearly spatially uniform and the power is deposited uniformly into the plasma bulk


Toneli et al., *J. Phys. D.*, **48** (2015) 325202 and Gudmundsson and Thorsteinsson, *PSST*, **16** (2007) 399

# *The global (volume averaged) model*

- The particle balance equation for a species $X$ is given as

$$\frac{\mathrm{d}n^{(X)}}{\mathrm{d}t} = 0 = \sum_i R^{(X)}_{\mathrm{Generation},i} - \sum_i R^{(X)}_{\mathrm{Loss},i}$$

  where $R^{(X)}_{\mathrm{Generation},i}$ and $R^{(X)}_{\mathrm{Loss},i}$, respectively, are the reaction rates of the various generation and loss processes of the species $X$

- Since the discharge is assumed to be quasi-neutral,

$$n_\mathrm{e} = \sum_\mathrm{i} Z_\mathrm{i} n_\mathrm{i}$$

  where $Z_\mathrm{i}$ is the charge of ion $\mathrm{i}$, an equation describing the particle balance of free electrons is not required

# *The global (volume averaged) model*

- To investigate the creation and destruction of species we compare the reaction rates
- The reaction rate $R$ for a given reaction is calculated as the product of the reactants, densities and the rate coefficient $k$ of the reaction,

$$R = k \times \prod_i n_{\mathrm{r},i} \qquad [\mathrm{m}^{-3}\mathrm{s}^{-1}]$$

  where $n_{\mathrm{r},i}$ is the density of the $i$-th reactant.
- The rate coefficient for electron impact reactions is

$$k = \langle v\sigma \rangle = 4\pi \int_0^\infty f(v)\sigma(v)v^3 \mathrm{d}v$$

# *The global (volume averaged) model*

- The power balance equation, equates the absorbed power $P_{\mathrm{abs}}$ to power losses due to elastic and inelastic collisions and losses due to charged particle flow to the walls is given as

$$\frac{1}{V}\left[P_{\mathrm{abs}} - eVn_{\mathrm{e}}\sum_{\alpha} n^{(\alpha)}\mathcal{E}_{\mathrm{c}}^{(\alpha)}k_{\mathrm{iz}}^{(\alpha)} - eu_{\mathrm{B0}}n_{\mathrm{i}}A_{\mathrm{eff}}(\mathcal{E}_{\mathrm{i}} + \mathcal{E}_{\mathrm{e}})\right] = 0$$

  where
  - $V$ is the volume of the discharge chamber
  - $A_{\mathrm{eff}} = 2\pi(R^2 h_L + RLh_R)$ is the effective area for ion loss
  - $u_{\mathrm{B0}} = \left[\frac{e\mathrm{T_e}}{m_{\mathrm{i}}}\right]^{1/2}$ is the Bohm velocity

# *The global (volume averaged) model*

- $\mathcal{E}_\mathrm{i} = V_\mathrm{p} + V_\mathrm{s}$ is the mean kinetic energy lost per ion lost
- $\mathcal{E}_\mathrm{e} = 2\mathrm{T_e}$ is the mean kinetic energy lost per electron lost
- $\mathcal{E}_\mathrm{c}^{(\alpha)}$ is the collisional energy loss per electron-ion pair created

$$\mathcal{E}_\mathrm{c}^{(X)} = \mathcal{E}_\mathrm{iz}^{(X)} + \sum_i \mathcal{E}_{\mathrm{ex},i}^{(X)} \frac{k_{\mathrm{ex},i}^{(X)}}{k_\mathrm{iz}^{(X)}} + \frac{k_\mathrm{el}^{(X)}}{k_\mathrm{iz}^{(X)}} \frac{3m_\mathrm{e}}{m^{(X)}} \mathrm{T_e}$$

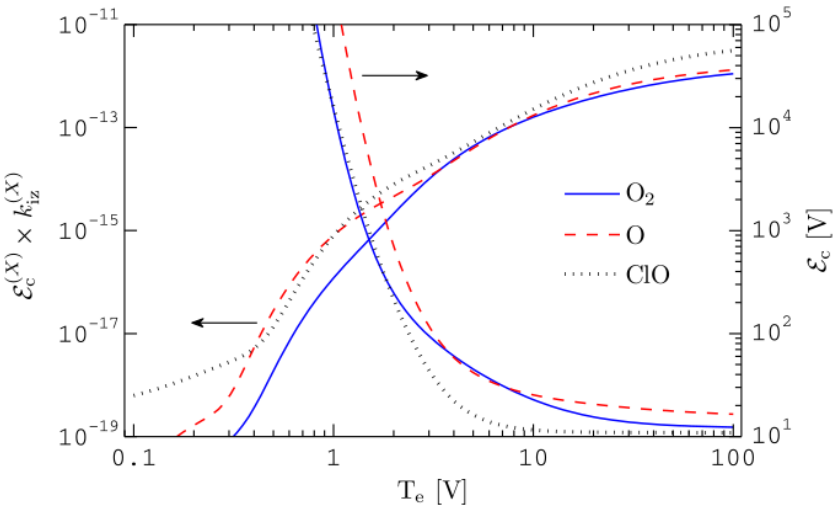

# *The global (volume averaged) model*

- For the edge-to-center positive ion density ratio we use

$$h_\ell \simeq \left[\left(\frac{0.86}{(3+\eta L/2\lambda_i)^{1/2}}\frac{1}{1+\alpha_0}\right)^2 + h_c^2\right]^{1/2}$$

$$h_R \simeq \left[\left(\frac{0.8}{(4+\eta R/\lambda_i)^{1/2}}\frac{1}{1+\alpha_0}\right)^2 + h_c^2\right]^{1/2}$$

where $\alpha_0 \approx (3/2)\alpha$ is the central electronegativity, $\eta = 2T_+/(T_+ + T_-)$ and

$$h_c \simeq \left[\gamma_-^{1/2} + \gamma_+^{1/2}\left[n_*^{1/2} n_+/n_-^{3/2}\right]\right]^{-1} \quad \text{and} \quad n_* = \frac{15}{56}\frac{\eta^2}{k_{rec}\lambda_i} v_i$$

is based on a one-region flat topped electronegative profile

$$\gamma_- = T_e/T_- \quad \text{and} \quad \gamma_+ = T_e/T_+$$

Kim et al., J. Vac. Sci. Technol. A, **24** (2006) 2025

# *The global (volume averaged) model*

- The electron energy distribution function (EEDF) is usually assumed to be Maxwellian
- We can also assume a general electron energy distribution

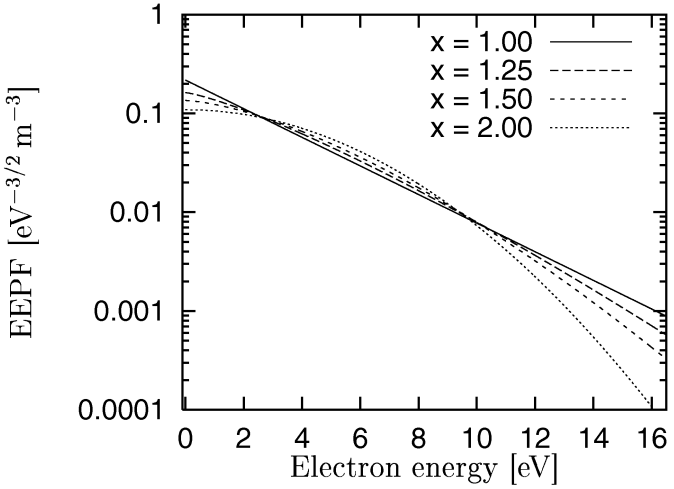


$$g_e(\mathcal{E}) = c_1 \mathcal{E}^{1/2} \exp\left(-c_2 \mathcal{E}^x\right)$$

$$c_1 = \frac{1}{\langle\mathcal{E}\rangle^{3/2}} \frac{[\Gamma(\xi_2)^{3/2}]}{[\Gamma(\xi_1)^{5/2}]} \quad \text{and} \quad c_2 = \frac{1}{\langle\mathcal{E}\rangle^{x}} \frac{[\Gamma(\xi_2)]}{[\Gamma(\xi_1)]^{x}}$$

where $\xi_1 = 3/2x$ and $\xi_2 = 5/2x$

$$g_p(\mathcal{E}) = \frac{g_e(\mathcal{E})}{\mathcal{E}^{1/2}}$$

- Here $x = 1$ and $x = 2$ correspond to Maxwellian and Druyvesteyn electron energy distributions, repectively

Gudmundsson *PSST*, **10** (2001) 76

# *The global (volume averaged) model*

- The diffusional losses of the neutral oxygen atoms (ground state and metastable) to the reactor walls are given by

$$k_{\mathrm{O,wall}} = \left[ \frac{\Lambda_{\mathrm{O}}^2}{D_{\mathrm{O}}} + \frac{2V(2-\gamma_{\mathrm{rec}})}{Av_{\mathrm{O}}\gamma_{\mathrm{rec}}} \right]^{-1} \quad \mathrm{s}^{-1}$$

  - $D_{\mathrm{O}}$ is the diffusion coefficient for oxygen atoms
  - $v_{\mathrm{O}} = (8eT_{\mathrm{g}}/\pi m_{\mathrm{O}})^{1/2}$ is the mean O velocity
  - $\gamma_{\mathrm{rec}}$ is the wall recombination coefficient for neutral oxygen atoms on the wall surface
  - $\Lambda_{\mathrm{O}}$ is the effective diffusion length of neutral oxygen atoms

$$\Lambda_{\mathrm{O}} = \left[ \left( \frac{\pi}{L} \right)^2 + \left( \frac{2.405}{R} \right)^2 \right]^{-1/2}$$

- The wall recombination coefficient $\gamma_{\mathrm{rec}}$ is one of the most important parameter in oxygen discharge modelling

# A.2.1 Model parameters

# *Surface recombination*

- The wall recombination probability, $\gamma_{\mathrm{rec}}$, is a very important quantity in all low pressure molecular discharges
- The pressure dependence on the wall recombination coefficient was achieved by fitting all the available data for stainless steel surfaces
- The same wall recombination coefficient was used for O($^1$D) as no data is available

Gudmundsson and Thorsteinsson, *PSST*, **16** (2007) 399

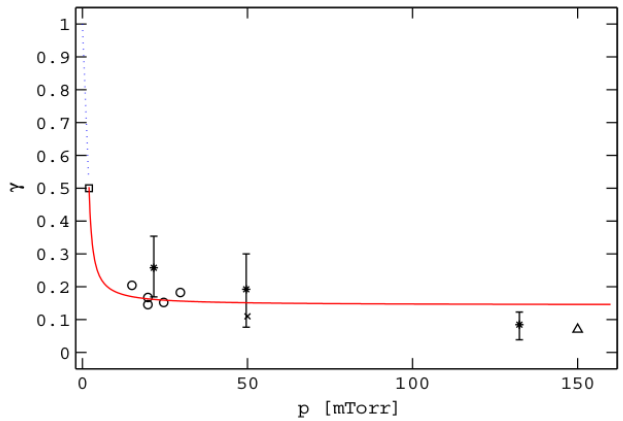


**Figure 1.** The recombination coefficient of oxygen atoms at the chamber walls for stainless steel as a function of pressure. The measured data is taken from, o Singh *et al* [47], × Matsushita *et al* [90], △ Mozetič and Zalar [91], □ Booth and Sadeghi [44] and ∗ Gomez *et al* [46]. The solid line shows a fit to the measured data and the dotted line is a linear extrapolation from $\gamma = 0.5$ at 2 mTorr to $\gamma = 1.0$ at vacuum.

The wall recombination coefficient for oxygen atoms on stainless steel surfaces depends on pressure through

$$\gamma_{\mathrm{rec}} = 0.1438 \exp(2.5069/p) \quad p > 2 \text{ mTorr}$$

$$\gamma_{\mathrm{rec}} = -0.25p + 1 \quad p < 2 \text{ mTorr}$$

# A.2.3 Particle densities


# *Particle densities – neutrals*

- The dominant species is the oxygen molecule in the ground state $O_2(X^3\Sigma_g)$ followed by the oxygen atom in the ground state $O(^3P)$
- The singlet metastable states $O_2(a^1\Delta_g)$ and $O_2(b^1\Sigma_g^+)$ and the metastable atom $O(^1D)$ are also present in the plasma in significant amounts
- a cylindrical stainless steel chamber

  radius $R$ = 15 cm and length $L$ = 30 cm $P_{abs}$ = 500 W

Toneli et al., *J. Phys. D*, **48** (2015) 325202

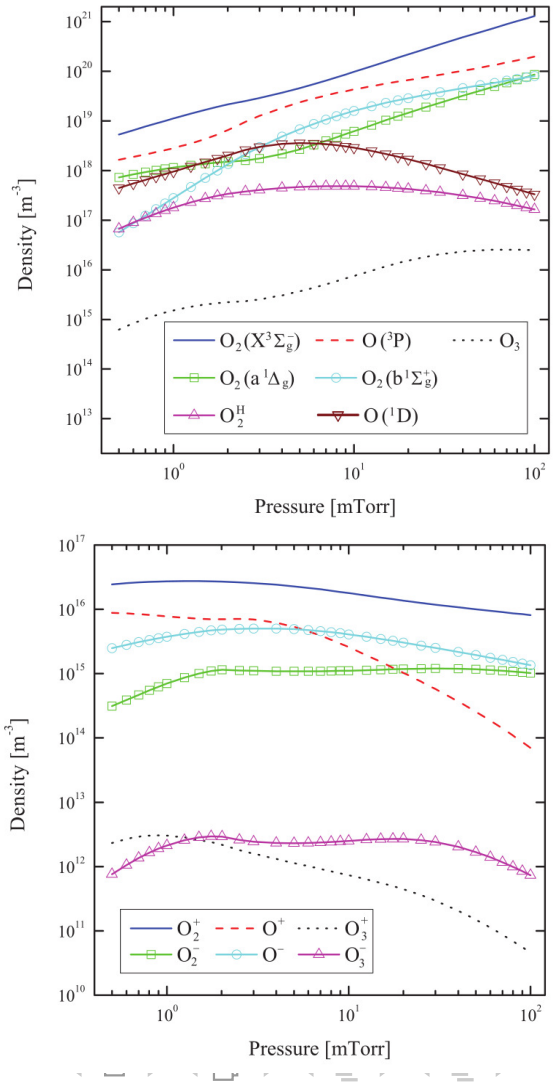

# *Particle densities – neutrals*

- The $O_2(b^1\Sigma_g^+)$ density overcomes the $O_2(a^1\Delta_g)$ density in the pressure range from 2.5 to 80 mTorr
- The $O_2^+$ ions are in majority among the positive ions
- The $O^+$ density has a sharp decrease for pressures above 4 mTorr
- The ratio $[O^-]/[O_2^-]$ is 5.3 at 1 mTorr, and 1.3 at 100 mTorr
- a cylindrical stainless steel chamber

  radius $R$ = 15 cm and length $L$ = 30 cm $P_{abs}$ = 500 W

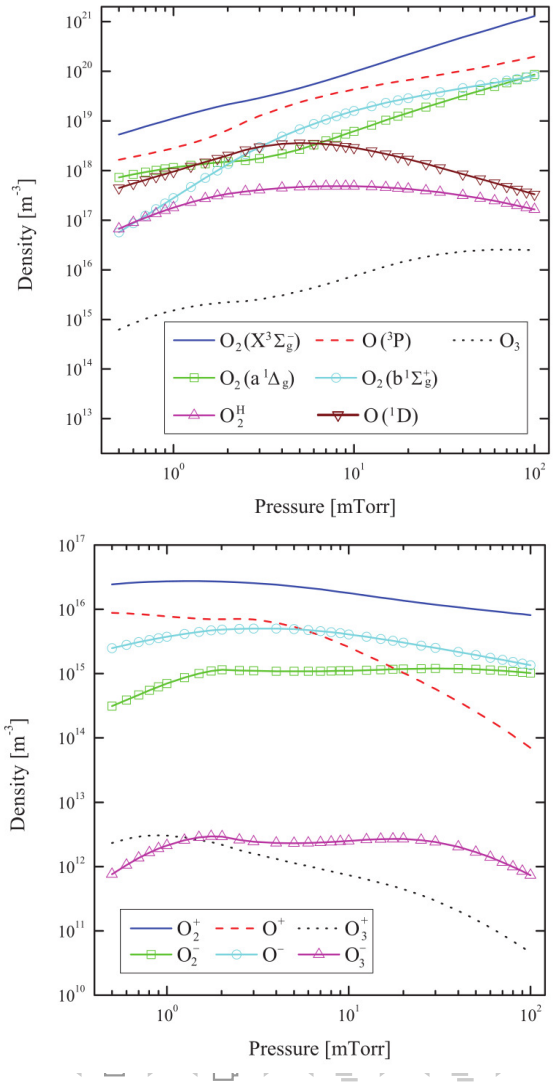


Toneli et al., *J. Phys. D*, **48** (2015) 325202

# *Particle densities – negative ions*

- $O^-$-ions are the dominating negative ions at low pressure
- The density of $O_2^-$ and $O_3^-$ is much smaller
- The importance of $O_2^-$-ions increases with increasing pressure
- Measurements of the negative ion densities in a capacitive rf discharge in the pressure range 70 – 350 mTorr indicate that $O_2^-$-ions are less than 2 % of all negative ions

Katsch et al., *PSST*, **9** (2000) 323

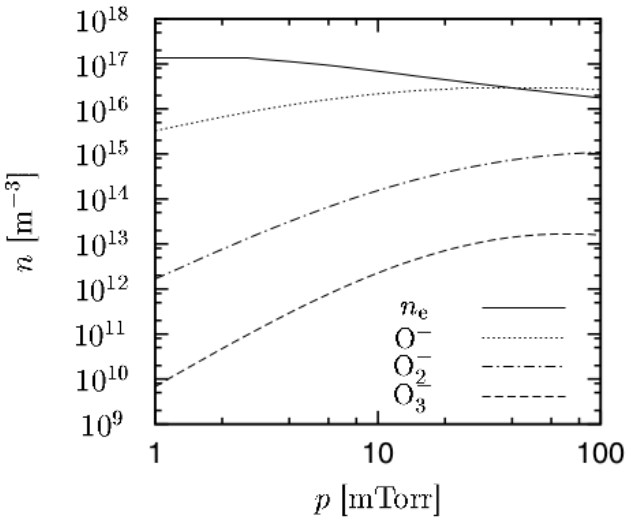


**Figure 6.** The densities of electrons $n_e$ and negative oxygen ions, $O^-$, $O_2^-$, and $O_3^-$, versus discharge pressure at 500 W and a flow rate of 50 sccm for a cylindrical stainless steel chamber with $L = 7.6$ cm and $R = 15.2$ cm.

Gudmundsson et al., *J. Phys. D*, **34** (2001) 1100

# *Particle densities – negative ions*

- The electronegativity

$$\alpha = \frac{n_- + n_{2-} + n_{3-}}{n_e}$$

  versus pressure
- The low pressure high density oxygen discharge is weakly electronegative
- The electronegativity decreases with increasing absorbed power

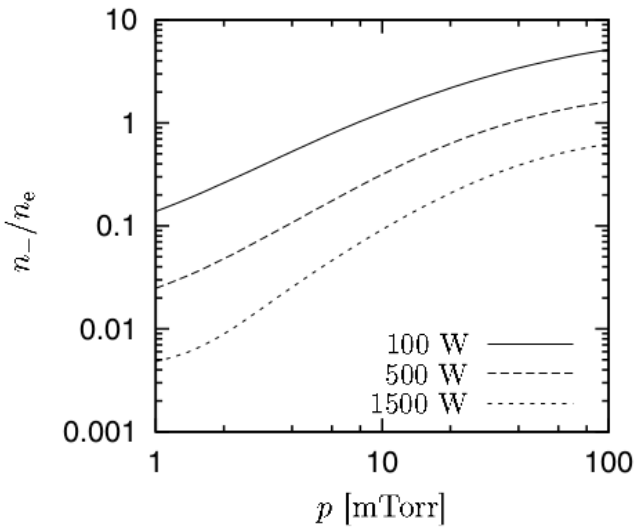


**Figure 7.** The electronegativity $n_e/(n_- + n_{2-} + n_{3-})$ at 100, 500 and 1500 W versus discharge pressure. We assume a flow rate of 50 sccm and a cylindrical stainless steel chamber with $L = 7.6$ cm and $R = 15.2$ cm.

Gudmundsson et al., *J. Phys. D*, **34** (2001) 1100

# *Creation of the negative ion $O^-$*

- Roughly half of the negative $O^-$-ions in a pure oxygen discharge are created through dissociative attachment from the metastable oxygen molecule $O_2(a^1\Delta_g)$:

$$e + O_2(a^1\Delta_g) \longrightarrow \begin{cases} O(^3P) + O^- \\ O(^1D) + O^- \end{cases}$$

at 10 mTorr and 500 W applied power

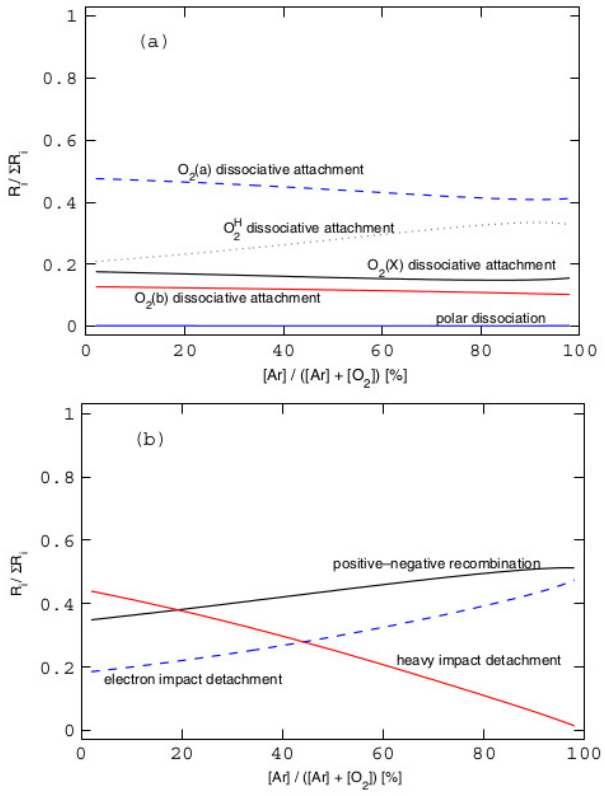


**Figure 10.** The reaction rates for (*a*) the creation of the $O^-$ ion and (*b*) the loss of the $O^-$ ion versus fractional argon flow rate [Ar]/([Ar] + [$O_2$]). The applied power is 500 W, the gas flow rate is 50 sccm and pressure is of 10 mTorr. The chamber is assumed to be made of stainless steel, cylindrical with $R = 10$ cm and $L = 10$ cm.

Gudmundsson and Thorsteinsson, *PSST*, **16** (2007) 399

# *Creation of the negative ion $O^-$*

- Roughly 20% are created through dissociative attachment from $O_2(A^3\Sigma_u^+, A^3\Delta_u, c^1\Sigma_u^-)$
- Dissociative attachment of the oxygen molecule is almost the sole source of $O^-$ in the discharge and the metastable oxygen molecules play a major role in the creation of negative ions

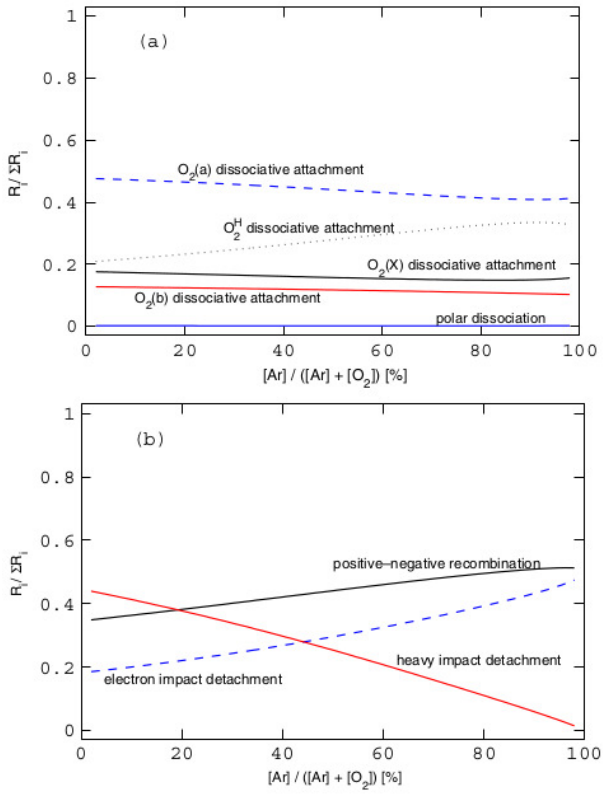


**Figure 10.** The reaction rates for (*a*) the creation of the $O^-$ ion and (*b*) the loss of the $O^-$ ion versus fractional argon flow rate [Ar]/([Ar] + [$O_2$]). The applied power is 500 W, the gas flow rate is 50 sccm and pressure is of 10 mTorr. The chamber is assumed to be made of stainless steel, cylindrical with $R = 10$ cm and $L = 10$ cm.

Gudmundsson and Thorsteinsson, *PSST*, **16** (2007) 399

# *Destruction of the negative ion $O^-$*

- At low pressure that the electron impact detachment (54),

$$e + O^- \longrightarrow O(^3P) + 2e$$

  is the main contributor to the loss of $O^-$
- Ion-ion mutual neutralization is also important (118, 119, 120) at low pressure
- As pressure increases, the contributions of these reactions become negligible

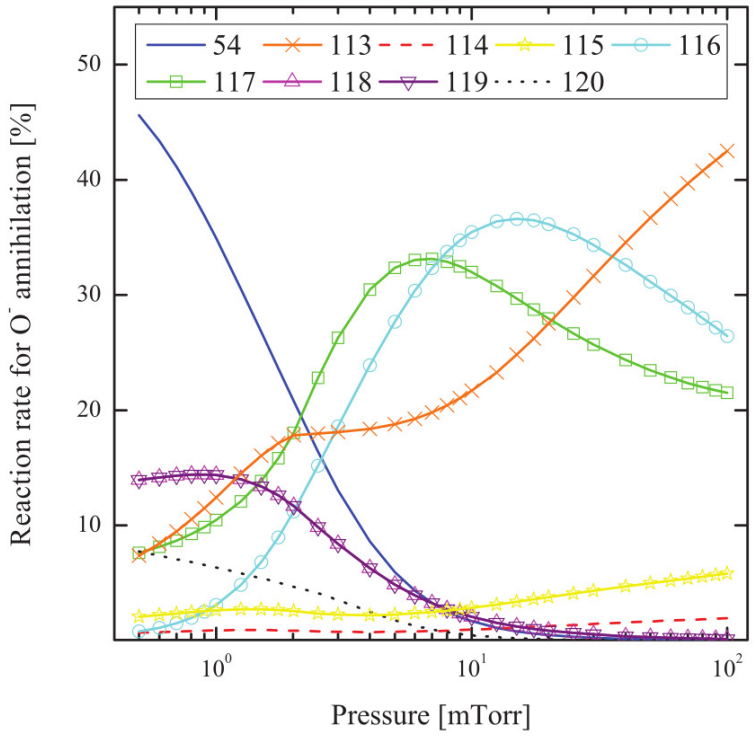


Toneli et al., *J. Phys. D*, **48** (2015) 325202

# *Destruction of the negative ion $O^-$*

- As the pressure increases charge exchange (113)

$$O^- + O_2(X^3\Sigma_g^-) \longrightarrow O(^3P) + O_2^-$$

and detachment by collision with $O(^3P)$ (117)

$$O^- + O(^3P) \longrightarrow O_2(X^3\Sigma_g^-) + e$$

have increased contribution as well as detachment by collision with $O_2(b^1\Sigma_g)$ (reaction 116)

$$O^- + O_2(b^1\Sigma_g) \longrightarrow O(^3P) + O_2(X^3\Sigma_g^-) + e$$

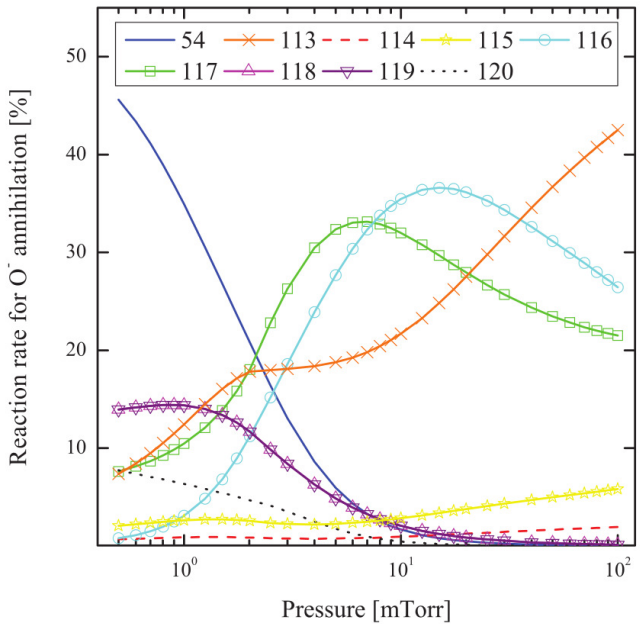


Toneli et al., *J. Phys. D*, **48** (2015) 325202

# *Creation of metastable $O_2(a^1\Delta_g)$ molecules*

- Electron impact excitation (17)

$$e + O_2(X^3\Sigma_g^-) \longrightarrow O_2(a^1\Delta_g) + e$$

has 100 % contribution at 1 mTorr and 68.2 % at 100 mTorr

- The role of quenching of the metastable atom $O(^1D)$ to create the metastable oxygen molecule (71)

$$O(^1D) + O_2(X^3\Sigma_g^-) \longrightarrow O_2(a^1\Delta_g) + O(^3P)$$

reaches a maximum value, 20.1 % contribution at 12.5 mTorr, and 10.5 % at 100 mTorr

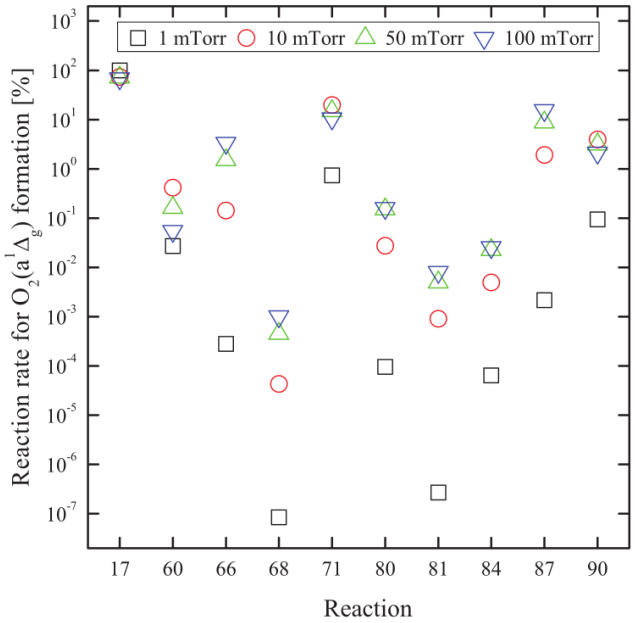


Toneli et al., *J. Phys. D*, **48** (2015) 325202

# *Destruction of metastable $O_2(a^1\Delta_g)$ molecules*

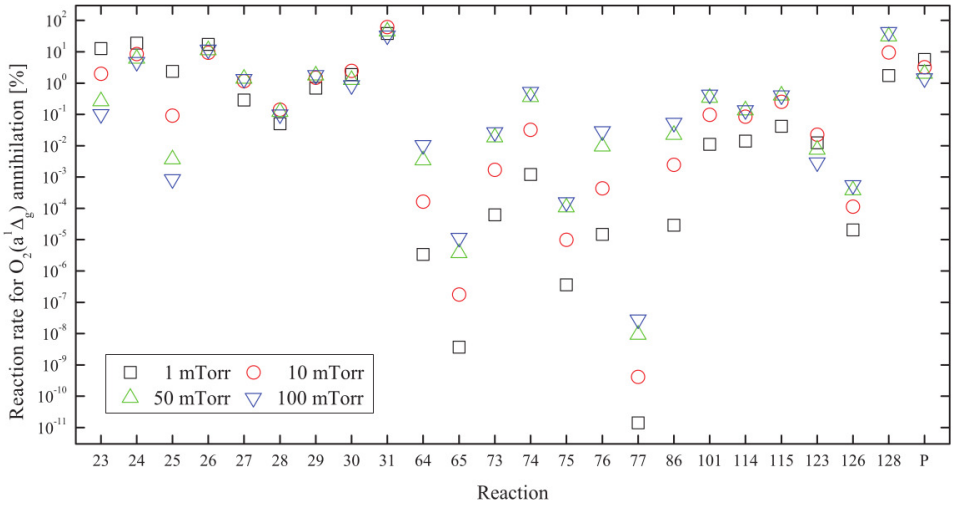


- Electron impact dissociation (31,24)

$$e + O_2(a^1\Delta_g) \longrightarrow O(^1D) + O(^3P) + e$$

$$e + O_2(a^1\Delta_g) \longrightarrow O(^3P) + O(^3P) + e$$

are the most important channels for destruction of the metastable $O_2(a^1\Delta_g)$ molecules, 57.2 % contribution at 1 mTorr and 38.1 % at 100 mTorr


Toneli et al., *J. Phys. D*, **48** (2015) 325202

# *Creation of metastable $O_2(b^1\Sigma_g)$ molecules*

- The most important contributor to the formation of the metastable oxygen molecule $O_2(b^1\Sigma_g)$ is reaction 72

$$O(^1D)+O_2(X^3\Sigma_g^-) \longrightarrow O_2(b^1\Sigma_g)+O(^3P)$$

  which has 75.7 % contribution at 1 mTorr and 93.2 % at 100 mTorr
- This reaction has been suggested in the past to be a major contributor to the formation of $b^1\Sigma_g^+$ state in the atmosphere

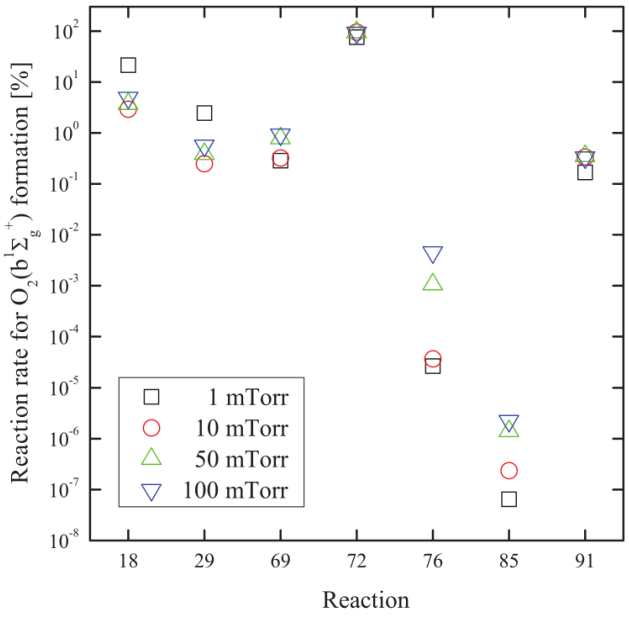


Toneli et al., *J. Phys. D*, **48** (2015) 325202

# *Destruction of metastable $O_2(b^1\Sigma_g)$ molecules*

- Wall quenching is an important loss process for $O_2(b^1\Sigma_g)$
- Electron impact dissociation (38,34)

$$e + O_2(b^1\Sigma_g) \longrightarrow O(^1D) + O(^3P) + e$$

$$e + O_2(b^1\Sigma_g) \longrightarrow O(^3P) + O(^3P) + e$$

are the most important channels for destruction along with electron impact ionization (33)

$$e + O_2(b^1\Sigma_g) \longrightarrow O_2^+ + 2e$$

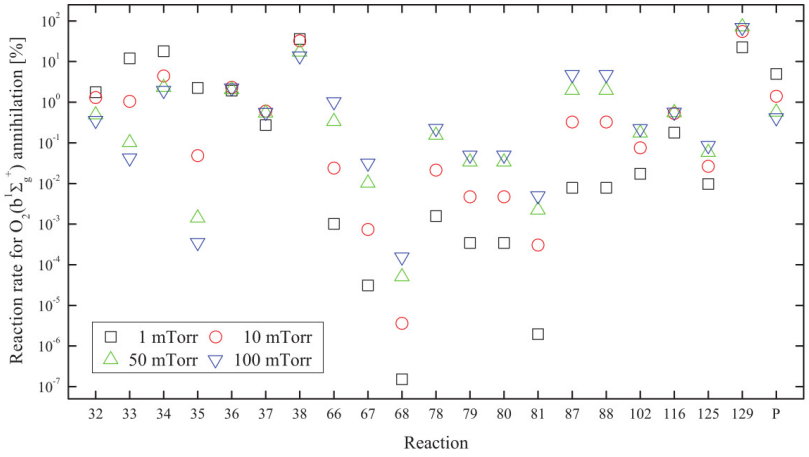


Toneli et al., *J. Phys. D*, **48** (2015) 325202

# A.2.4 Influence of chamber wall and EEDF


# *Influence of chamber wall and EEDF*

- The parameter $x$ defines the shape of the electron energy distribution
  - $x = 0.5$ is concave or bi-Maxwellian
  - $x = 1$ is a Maxwellian distribution
  - $x = 2$ is Druyvesteyn distribution
- For anodized aluminium reactor walls, the recombination coefficient for oxygen atoms at the walls is assumed to be a constant $\gamma_O = 0.06$ based on the measurements of Guha et al. (2008)
- The chamber wall has a significant influence on the dissociation fraction

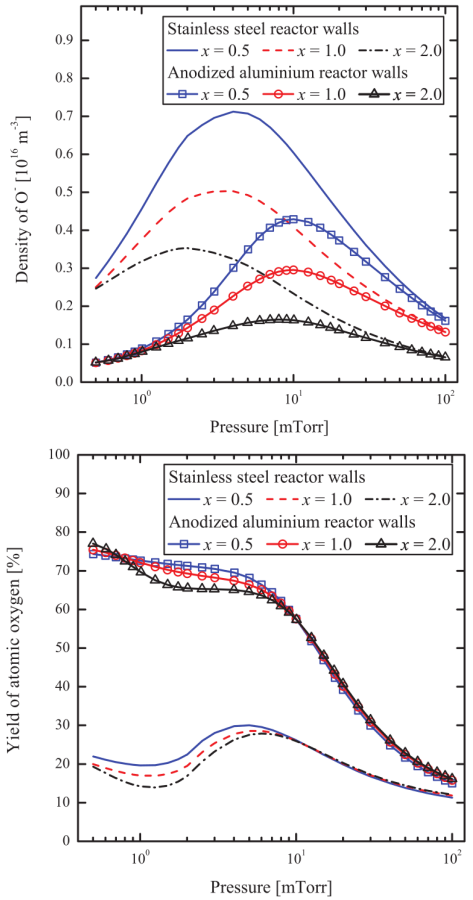


Toneli et al., *J. Phys. D*, **48** (2015) 495203

# A.2.5 Chlorine dilution

# *Chlorine dilution – Particle densities*

- The chlorine-oxide molecule ClO and its ion $ClO^+$ peak when $Cl_2$ and $O_2$ flowrates are roughly equal
- The $O_2(a^1\Delta_g)$ density is about 9 – 10 % of the total $O_2$ density
- The electron density increases about 30 % between pure chlorine and pure oxygen discharge

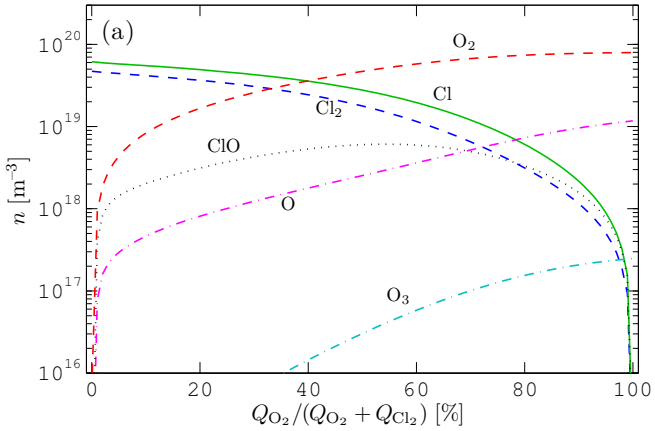


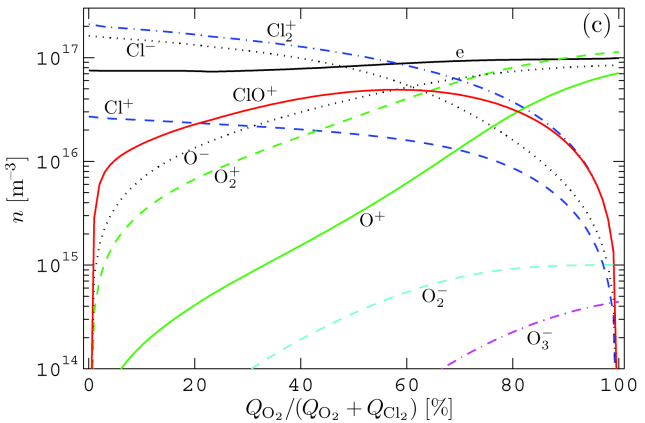


Thorsteinsson and Gudmundsson, *Plasma Sources Sci. Technol.*, **19** 055008 (2010)

A cylindrical stainless steel chamber
$L$ = 10 cm and $R$ = 10 cm
$p$ = 10 mTorr and $P_{abs}$ = 500 W

# *Oxygen dilution – Particle densities*

- The total rate for creation and loss of ClO molecules is at maximum when the oxygen content is 65%
- Wall recombination of Cl molecules, is the dominating pathway for creation of ClO molecules
- The bulk processes and recombination of $ClO^+$ ions at the wall account for roughly 33–43% of the total rate for ClO creation, combined

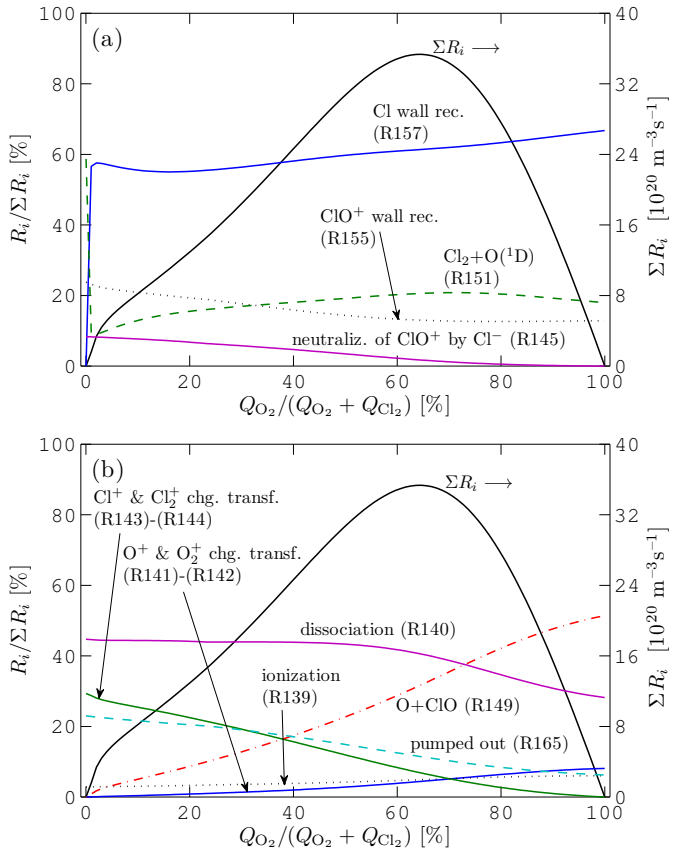


Thorsteinsson and Gudmundsson, *Plasma Sources Sci. Technol.*, **19** 055008 (2010)

# A.3 Summary

# *Summary*

- A global model of $O_2$, and $Cl_2/O_2$ discharges has been applied to explore the creation and destruction of the singlet metastable molecules $O_2(a^1\Delta_g)$, $O_2(b^1\Sigma_g^+)$
- The singlet delta state $O_2(a^1\Delta_g)$ is created mainly by lectron impact excitation

$$e + O_2(X^3\Sigma_g^-) \longrightarrow O_2(a^1\Delta_g) + e$$

- The singlet delta state $O_2(b^1\Sigma_g^+)$ is created mainly by

$$O(^1D) + O_2(X^3\Sigma_g^-) \longrightarrow O_2(b^1\Sigma_g) + O(^3P)$$

- At low pressure that the electron impact detachment

$$e + O^- \longrightarrow O(^3P) + 2e$$

  is the main contributor to the loss of $O^-$
- The ClO molecule is mainly created by recombination at the discharge wall

# B. 1D particle-in-cell/Monte Carlo collision simulation


# *Introduction*

- B.1 The 1D particle-in-cell/Monte Carlo collision simulation
  - The oxygen discharge
  - Capacitively Coupled Oxygen Discharge at 13.56 MHz
    - pressure dependence
    - driving frequency dependence
    - surface quenching of $O_2(a^1\Delta_g)$
    - the effect of $\gamma_{\mathrm{see}}(\mathcal{E})$
  - Summary

# *Introduction*

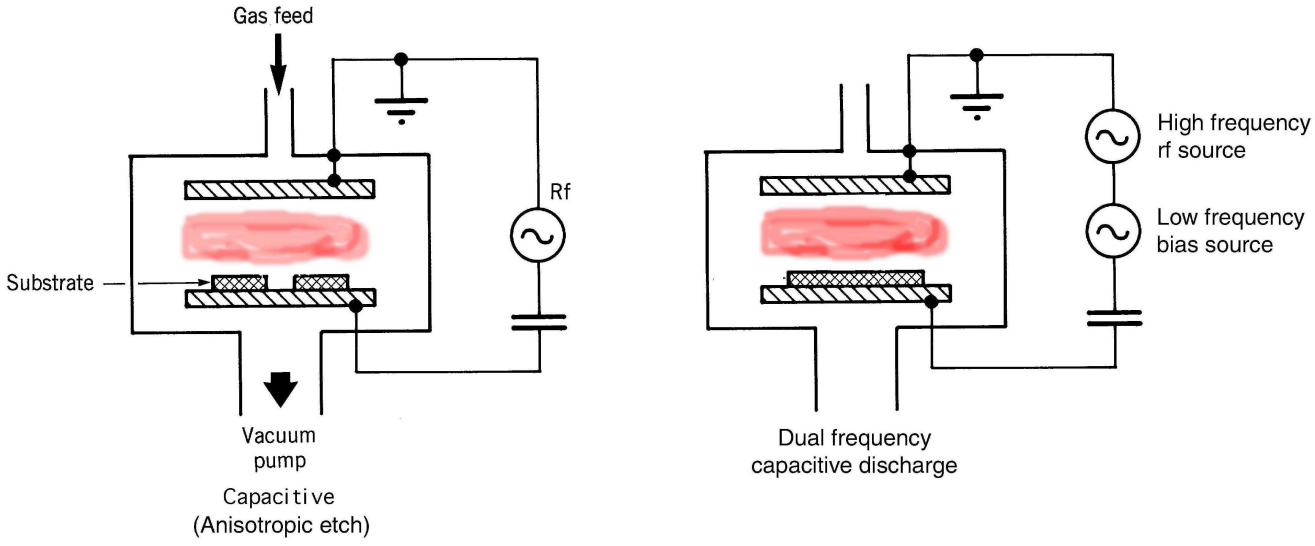


- One of the most widely used types of low-pressure discharges is sustained by radio-frequency (rf) currents and voltages, introduced through a capacitive sheaths
- The currents in the main body of the plasma lead to Ohmic heating, while the voltage across the sheath leads to stochastic sheath heating

# The 1D particle-in-cell/Monte Carlo collision simulation


# *The oopd1 1d-3v PIC/MCC code*

- In particle-in-cell simulation the plasma is represented as a collection of macroparticles
- Each macroparticle is a charged “cloud” representing many real charged particles
- Each macroparticle has the same charge-to-mass ratio ($q/m$) as the real charged particle
- Equations of motion are solved for each macroparticle
- The electric and magnetic fields are calculated self-consistently using charge densities and currents produced by the macroparticles

# *The oopd1 1d-3v PIC/MCC code*

- We use the `oopd1` (objective oriented plasma device for one dimension) code to simulate the discharge
- The `oopd1` code was originally developed at the Plasma Theory and Simulation Group at UC Berkeley
- It has 1 dimension in space and 3 velocity components for particles (1d-3v)
- The `oopd1` code is supposed to replace the widely used `xpdx1` series (`xpdp1`, `xpdc1` and `xpds1`)
- It is developed to simulate various types of plasmas, including processing discharges, accelerators and beams
  - Modular structure
  - Includes relativistic kinematics
  - Particles can have different weights

Gudmundsson et al., *Plasma Sources Sci. Technol.*, **22** 035011 (2013)

# B.2. The oxygen discharge

# *The oxygen discharge*

- We consider a discharge that consists of:
  - electrons
  - the ground state oxygen molecule $O_2(X^3\Sigma_g^-)$
  - the metastable oxygen molecule $O_2(a^1\Delta_g)$
  - the metastable oxygen molecule $O_2(b^1\Sigma_g)$
  - the ground state oxygen atom $O(^3P)$
  - the metastable oxygen atom $O(^1D)$
  - the negative oxygen ion $O^-$
  - the positive oxygen ions $O^+$ and $O_2^+$
- The discharge model includes energy dependent secondary electron emission yield
- We assume a parallel plate capacitively coupled oxygen discharge at with electrode separation of 4.5 cm
- We apply a global model[1] beforehand to calculate the partial pressure of the various neutrals

[1] Thorsteinsson and Gudmundsson, *Plasma Sources Sci. Technol.*, **19** 055008 (2010)

# *The oxygen discharge*

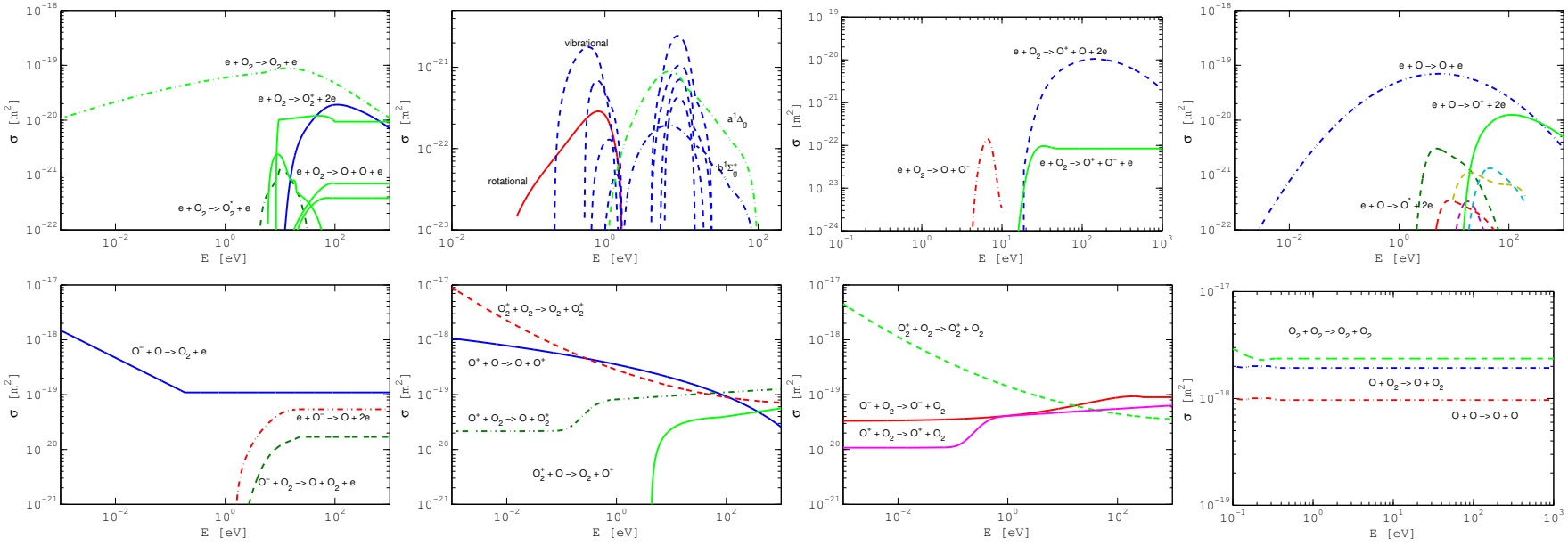


- The reaction set for the oxygen is comprehensive and for this study includes 67 reactions


Gudmundsson et al., *Plasma Sources Sci. Technol.*, **22** 035011 (2013)

Gudmundsson and Lieberman, *Plasma Sources Sci. Technol.*, **24** 035016 (2015)

Hannesdottir and Gudmundsson, *Plasma Sources Sci. Technol.*, **25** 055002 (2016)

# Capacitively Coupled Oxygen Discharge single frequency at 13.56 MHz

## – pressure dependence –

## including $O_2(a^1\Delta_g)$ with $\gamma_{see} = 0.0$

# *Oxygen CCP – pressure dependence*

- We apply a voltage source with a single frequency

$$V(t) = V_{\mathrm{rf}} \sin(2\pi f t)$$

- The electrodes are circular with a diameter of 14.36 cm
- The gap between the electrodes is 4.5 cm
- We set $V_{\mathrm{rf}} = 222$ V and $f = 13.56$ MHz
- The neutrals ($O_2$ and O) are treated as background gas at $T_{\mathrm{g}} = 300$ K with a Maxwellian distribution
- The dissociation fraction and the metastable fraction is found using a global model
- The pressure is varied from 10 – 500 mTorr

# *Oxygen CCP – pressure dependence*

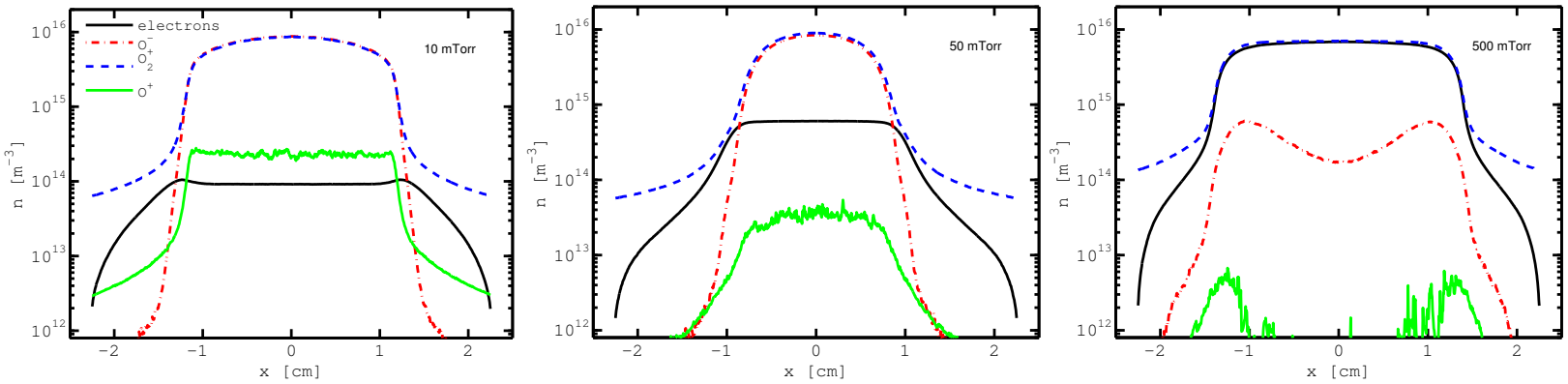


- For a parallel plate capacitively coupled oxygen discharge at 10, 50 and 500 mTorr with with a gap separation of 4.5 cm by a 222 V voltage source at 13.56 MHz
  - $O_2^+$-ion density profile
  - $O^+$-ion density profile
  - $O^-$-ion density profile
  - electron density profile

Gudmundsson and Ventéjou (2015) JAP **118** 153302

# *Oxygen CCP – pressure dependence*

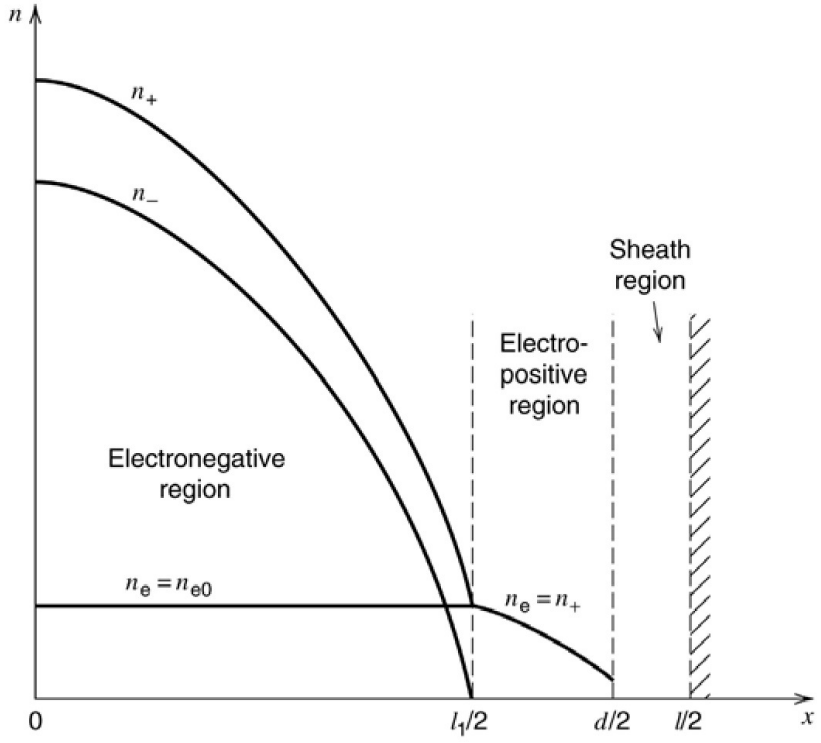


Lieberman and Lichtenberg (2005)

- In the electronegative discharge the plasma tends to stratify into an electronegative core and electropositive edge

# *Oxygen CCP – pressure dependence*

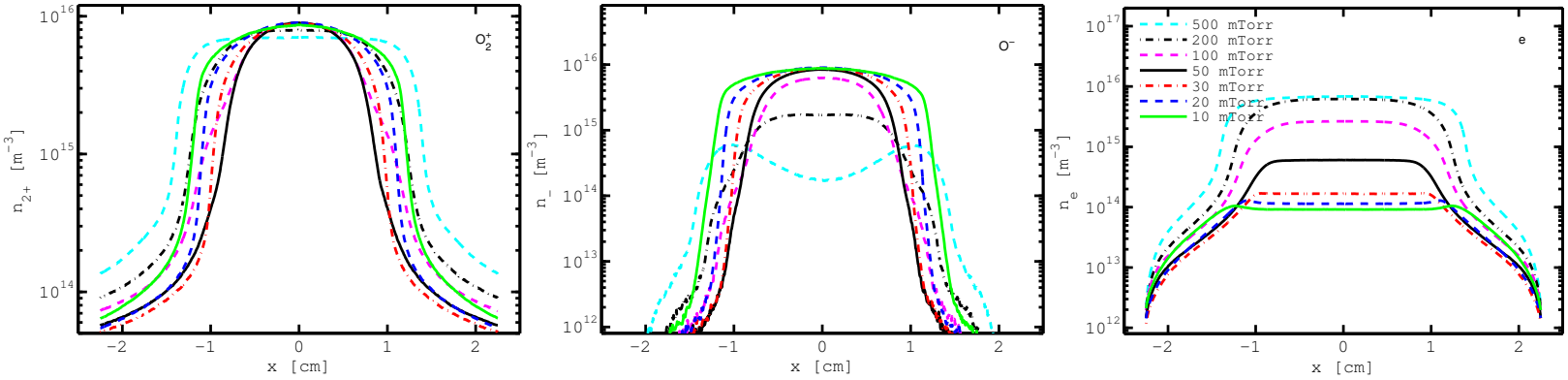


- The sheath width decreases as the pressure is decreased in the pressure range from 50 mTorr to 10 mTorr
- The sheath widths are largest at 50 mTorr
- As the pressure is increased from 50 mTorr up to 500 mTorr the sheath width decreases
- This agrees with what has been observed experimentally in the pressure range 40 – 375 mTorr

Mutsukura et al. (1990) JAP **68** 2657 and van Roosmalen et al. (1985) JAP **58** 653

# *Oxygen CCP – pressure dependence*

- The electron heating profile $\mathbf{J}_e \cdot \mathbf{E}$
- In the pressure range 50 - 500 mTorr the electron heating occurs almost solely in the sheath region
- As the pressure is decreased the Ohmic heating contribution in the plasma bulk increases and sheath heating decreases

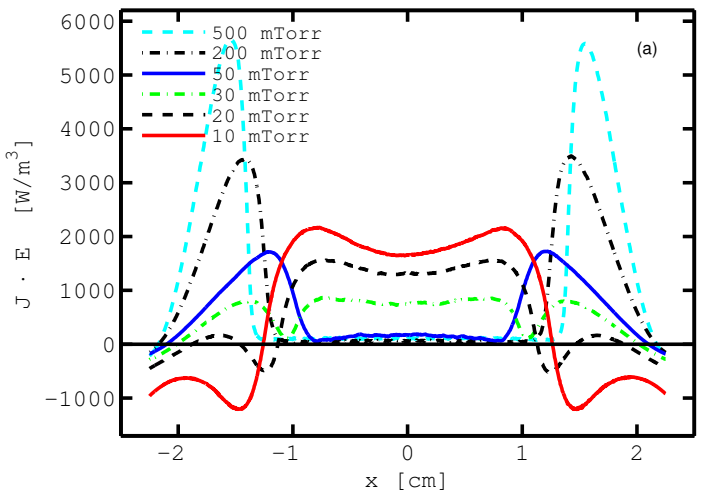


Gudmundsson and Ventéjou (2015) JAP **118** 153302

# *Oxygen CCP – pressure dependence*

- At **10 mTorr** excluding the metastable states in the simulation has very small influence on the heating mechanism
- At **50 mTorr** the metastable states have a significant influence on the heating mechanism
- The role of the metastables is even more significant at **200 mTorr**

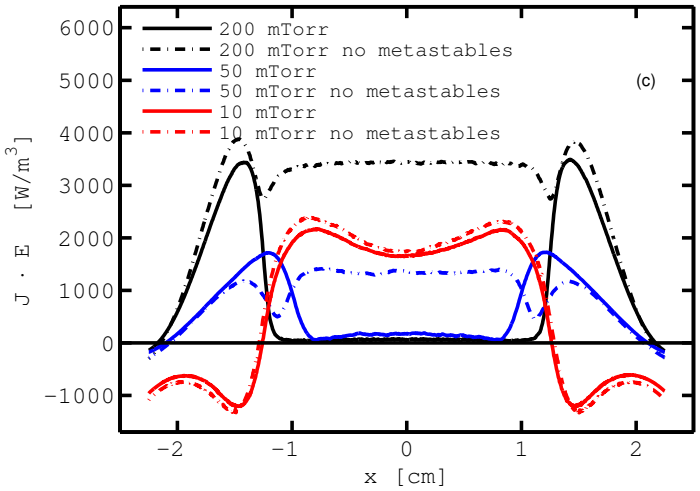


Gudmundsson and Ventéjou (2015) JAP **118** 153302

Gudmundsson and Lieberman (2015) PSST **24** 035016

# *Oxygen CCP – pressure dependence*

- At low pressure the EEPF curves outwards, the population of low energy electrons is relatively low
- As the pressure is increased the number of low energy electrons increases and the number of higher energy electrons (> 10 eV) decreases
- Thus the EEPF curves inwards or becomes bi-Maxwellian as the pressure is increased

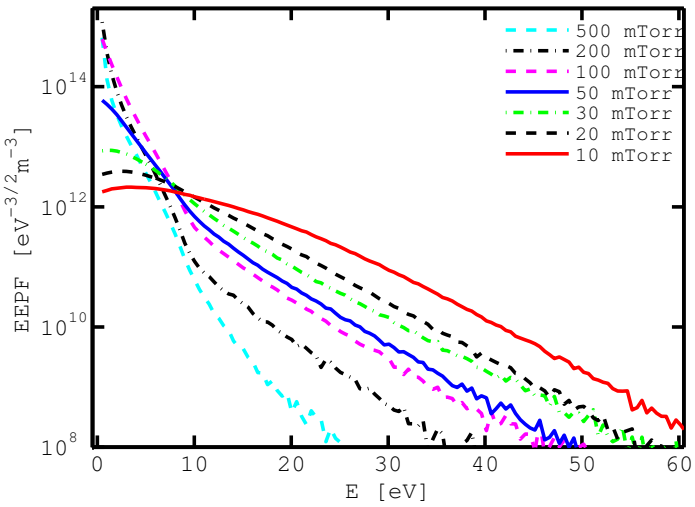


Gudmundsson and Ventéjou (2015) JAP **118** 153302

# *Oxygen CCP – pressure dependence*

- Our results agree with the measurements of Lee et al. (2010) which explored experimentally the evolution of the EEPF with pressure in a capacitively coupled oxygen discharge in the pressure range 3 – 100 mTorr
- They find that the EEPF became more distinctly bi-Maxwellian and the density of low energy electrons increases as the gas pressure is increased

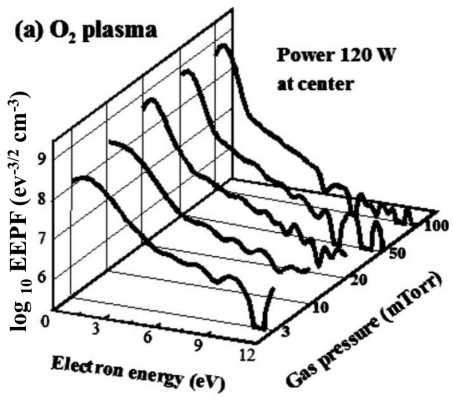


Lee et al. (2010) PRE **81** 046402

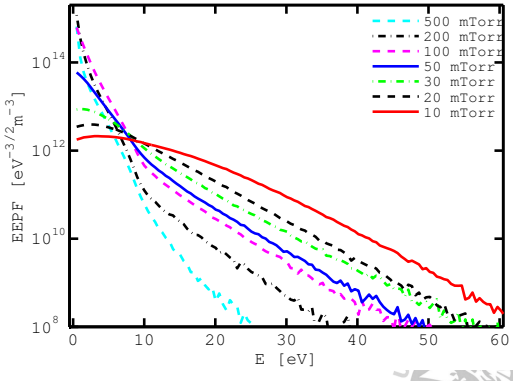


Gudmundsson and Ventéjou (2015) JAP **118** 153302

# *Oxygen CCP – pressure dependence*

- The effective electron temperature drops as the pressure is increased
- When the metastable singlet oxygen molecule $O_2(a^1\Delta_g)$ is added to the discharge model the effective electron temperature drops, in particular in the electronegative core due to detachment by the metastable $O_2(a^1\Delta_g)$ molecule

$$O^- + O_2(a^1\Delta_g) \rightarrow \text{products}$$

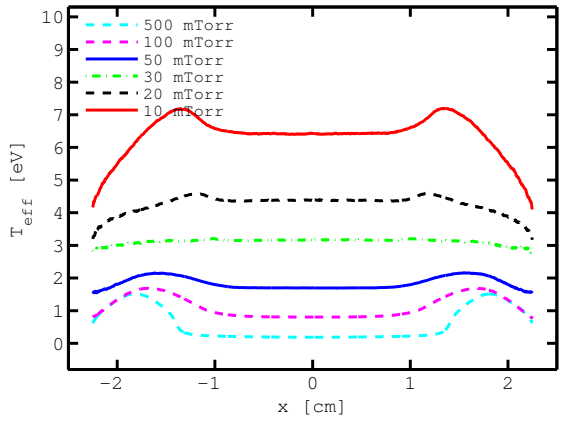


Gudmundsson and Ventéjou (2015) JAP **118** 153302

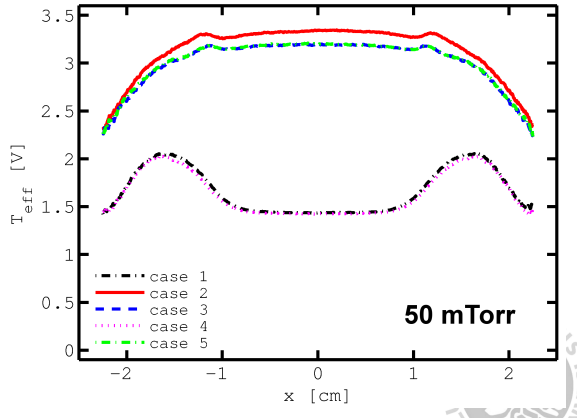


Gudmundsson and Lieberman (2015) PSST **24** 035016

# *Oxygen CCP – pressure dependence*

- At low pressure the EEPF curves outwards and develops an inward curving shape or becomes bi-Maxwellian as the pressure is increased
- These results contradict what is commonly found for the capacitively coupled argon discharge where the EEPF evolves from being bi-Maxwellian at low pressure to being more Druyvesteyn like at high pressure

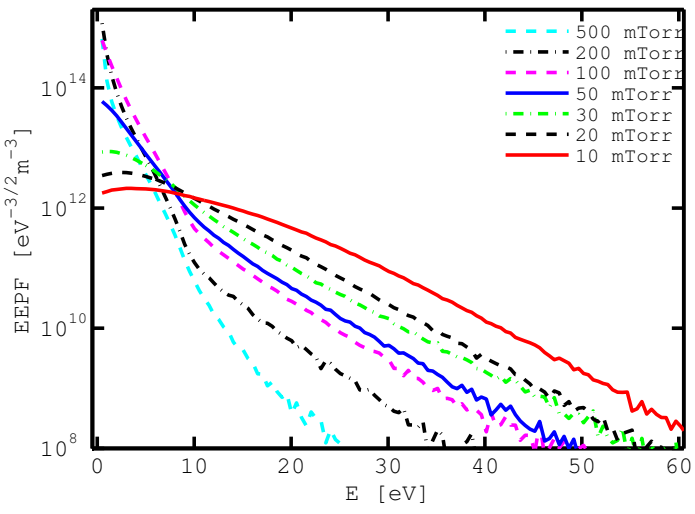


Gudmundsson and Ventéjou (2015) JAP **118** 153302

Godyak and Piejak (1990) Phys. Rev. Lett. **65** 996

Vahedi et al. (1993) Plasma Sources Sci. Technol. **2** 273

# Capacitively Coupled Oxygen Discharge single frequency at 13.56 MHz

## – pressure dependence –

## including $O_2(a^1\Delta_g)$, $O_2(b^1\Sigma_g)$ and $\gamma_{see}(\mathcal{E})$


# *Oxygen CCP – pressure dependence*

- It has been known for decades that the metastable oxygen molecule $O_2(b^1\Sigma_g)$ plays an important role in the oxygen discharge

  Thompson (1961) *Proc. Royal Soc. A 262*(1311) 519

- Recent global model study indicates there is a significant density of $O_2(b^1\Sigma_g)$ in the oxygen discharge
- The $O_2(b^1\Sigma_g)$ is mainly created through

$$O_2(X^3\Sigma_g^-) + O(^1D) \longrightarrow O_2(b^1\Sigma_g) + O(^3P)$$

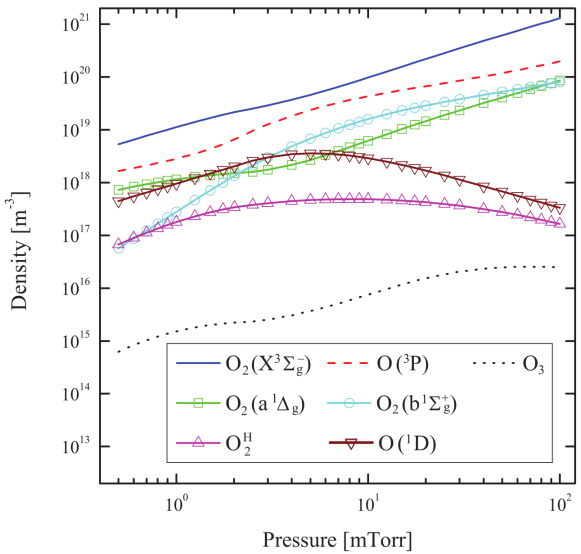


Toneli et al., *J. Phys. D*, **48** 325202 (2015)

# *Oxygen CCP – pressure dependence*

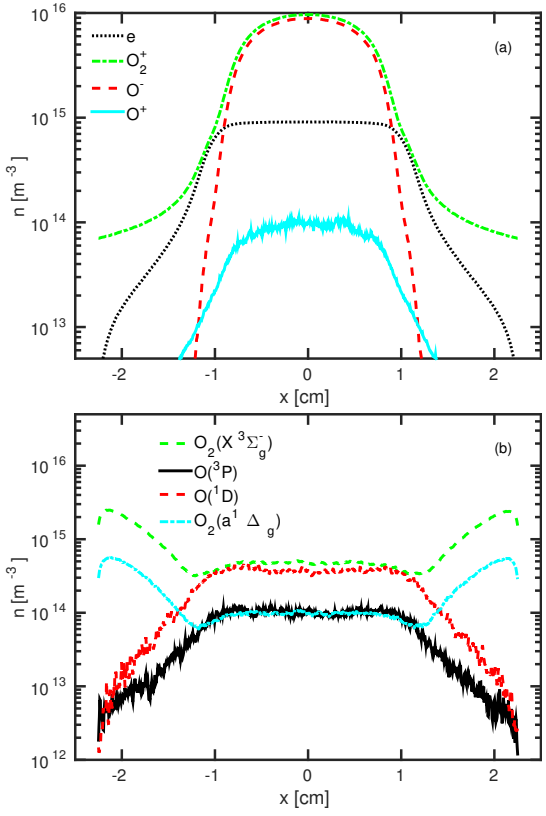


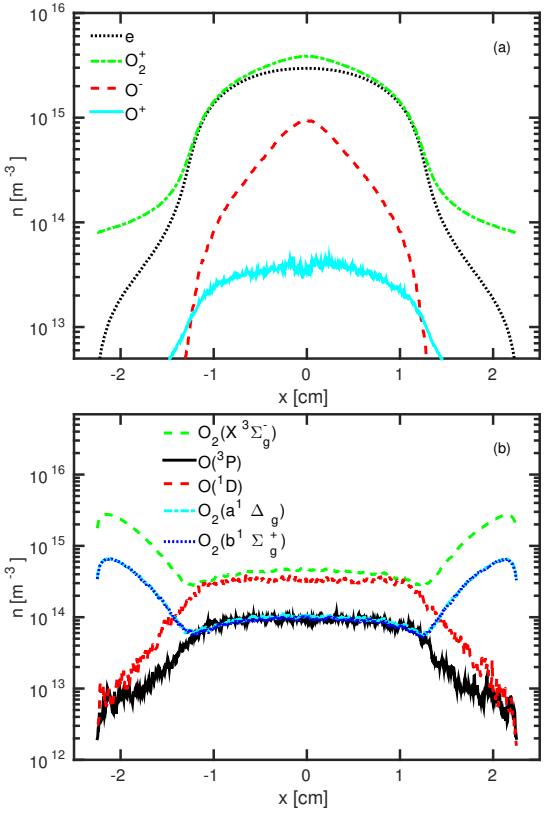


- The density profiles of charged particles and fast neutrals comparing including $O_2(a^1\Delta_g)$ (left) and $O_2(a^1\Delta_g)$ and $O_2(b^1\Sigma_g)$ (right) at 50 mTorr

# *Oxygen CCP – pressure dependence*

- The number of cold electrons increases and negative ion density decreases as the metastables $O_2(a^1\Delta_g)$ and $O_2(b^1\Sigma_g)$ are added to the discharge model
- The electron heating in the bulk drops to zero at the higher pressures
- The effective electron temperature profile changes significantly when detachment by singlet metastables is added to the reaction set
- **10 mTorr**, **50 mTorr** and **200 mTorr**

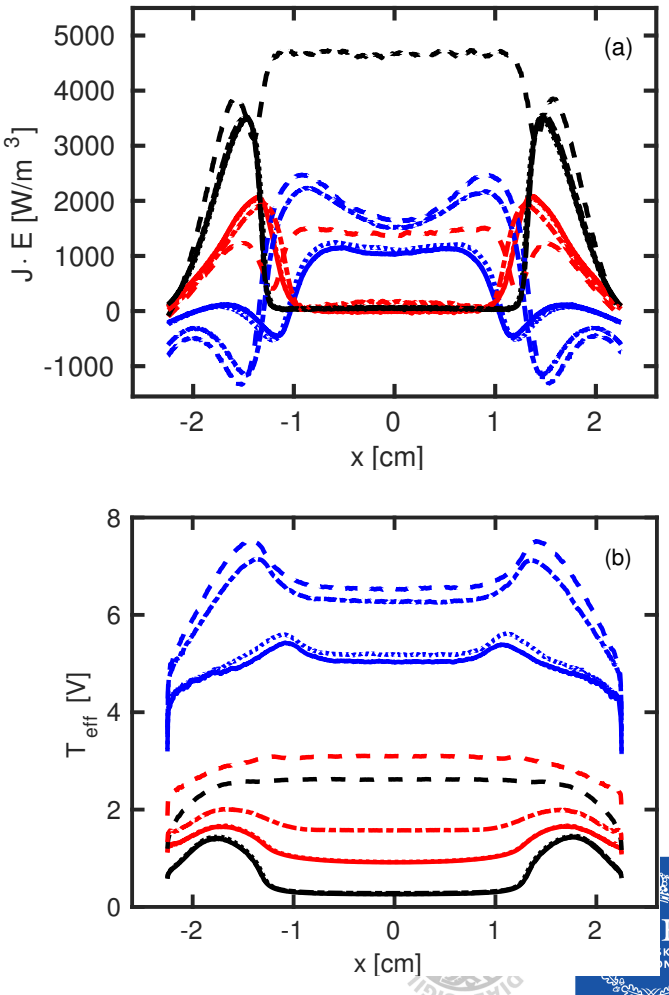


Gudmundsson and Hannesdottir, AIP Conf. Proc. **1811** 120001 (2017)

# *Oxygen CCP – pressure dependence*

- We have compiled experimental data from the literature on secondary electron emission yields for the species $O_2^+$, $O^+$, $O_2$ and O bombarding various metals and substances
- A fit was made through the available experimental data

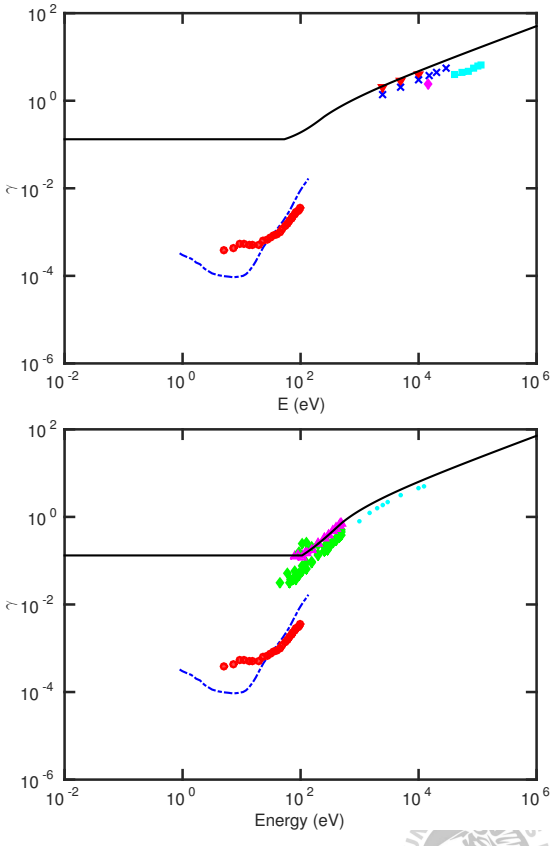

# *Oxygen CCP – pressure dependence*

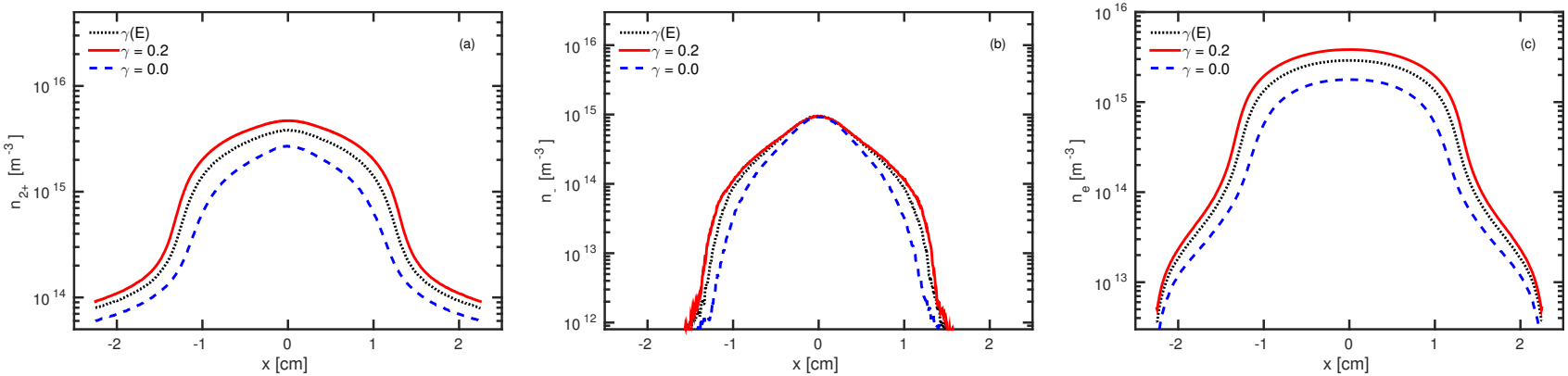


- The $O_2^+$, $O^-$ and electron density profiles for $\gamma_{see} = 0.0$, $\gamma_{see} = 0.2$, and energy dependent secondary electron emission yield
- The electron density increases with increased secondary electron emission yield

# *Oxygen CCP – pressure dependence*

- Comparison to experimental findings:
  - o $\gamma_{see} = 0.0$,
    4.4 % $O_2(a^1\Delta_g)$
  - \+ $\gamma_{see} = 0.0$,
    4.4 % $O_2(a^1\Delta_g)$ and 4.4 % $O_2(b^1\Sigma_g)$
  - x $\gamma_{see} = \gamma_{see}(E)$,
    4.4 % $O_2(a^1\Delta_g)$ and 4.4 % $O_2(b^1\Sigma_g)$
  - ▪ Experimental findings by Kechkar

    (S. Kechkar, Ph.D. Thesis, Dublin City University, January 2015)

Hannesdottir and Gudmundsson (2016) PSST **25** 055002

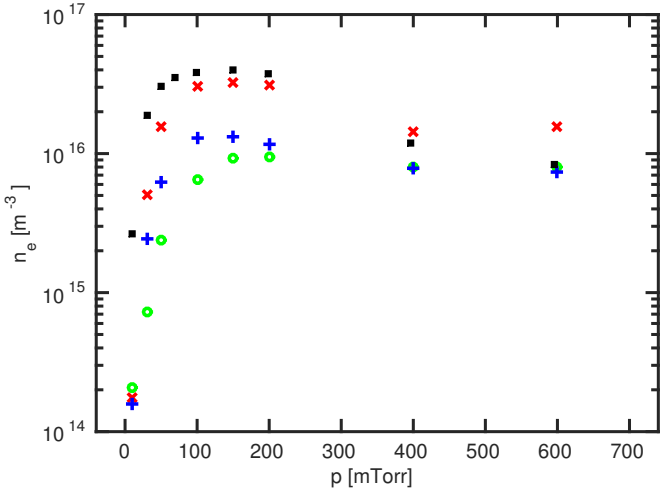


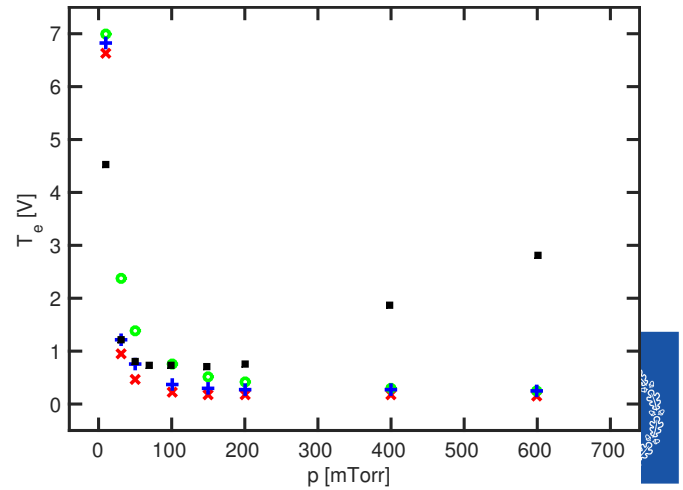

# *Oxygen CCP – pressure dependence*

- The spatio-temporal electron heating $\mathbf{J}_e \cdot \mathbf{E}$ at 10 and 50 mTorr
- At 10 mTorr there is a significant electron heating within the electronegative core
- At 50 mTorr the electron heating occurs almost solely in the sheath region

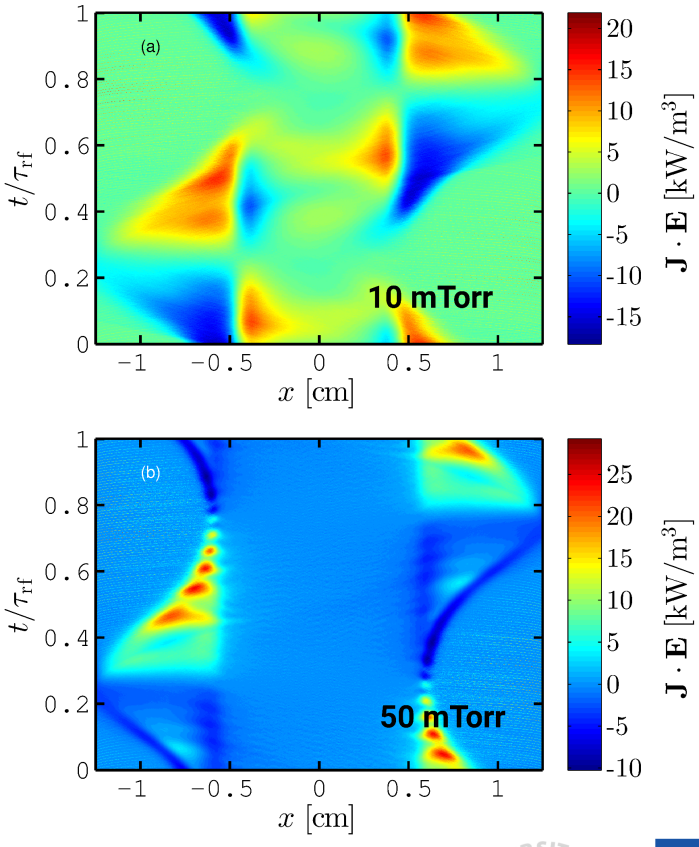


Hannesdottir and Gudmundsson (2016) PSST, **25** 055002

Gudmundsson and Ventéjou (2015) JAP **118** 153302

Gudmundsson and Snorrason (2017) JAP **122** 193302

# *Oxygen CCP – pressure dependence*

- The time averaged electron heating $\langle \mathbf{J}_e \cdot \mathbf{E} \rangle$ at 10 and 50 mTorr
- At 10 mTorr there is significant electron heating within the electronegative core
- At 50 mTorr, the heating rate in the electronegative core is roughly zero, and electron heating is almost entirely located in the sheath regions

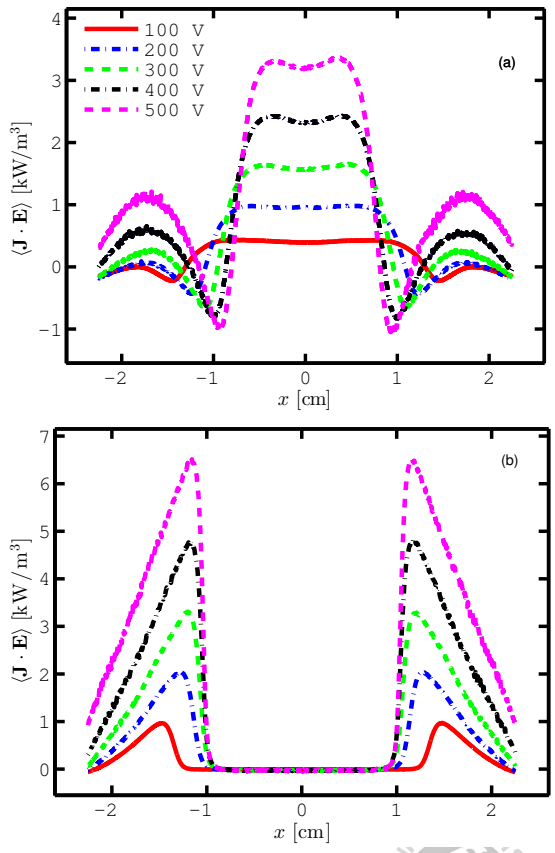


Gudmundsson and Snorrason (2017) JAP **122** 193302

# *Oxygen CCP – pressure dependence*

- At 10 mTorr the effective electron temperature is high within the plasma bulk (the electronegative core) throughout the rf period and peaks within the plasma bulk during the sheath collapse phase
- At 50 mTorr a peak in the effective electron temperature within the plasma bulk in the sheath expansion phase and is low within the plasma bulk throughout the rf period

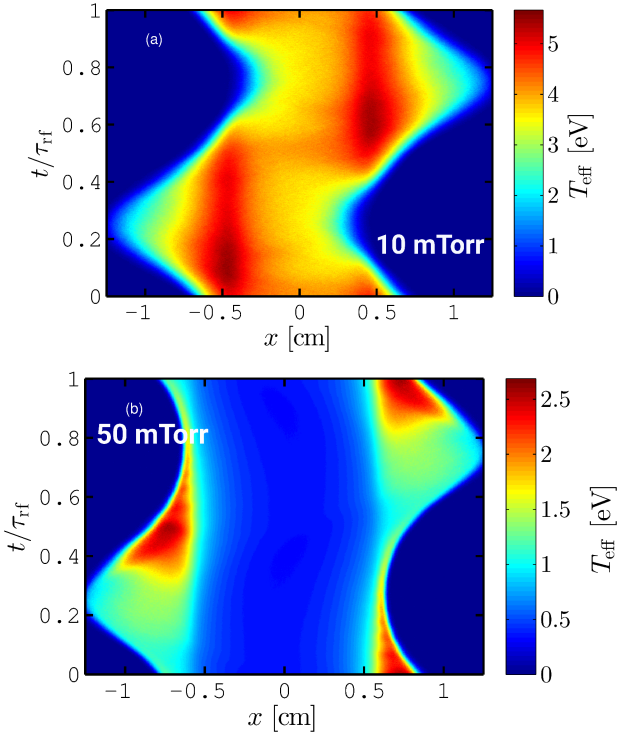


Gudmundsson and Snorrason (2017) JAP **122** 193302

# *Oxygen CCP – pressure dependence*

- The axial electric field at $t/\tau_{\mathrm{rf}} = 0.5$ for both 10 and 50 mTorr
- At 10 mTorr there is a significant electric field strength within the electronegative core
- This strong electric field within the plasma bulk (the electronegative core) indicates a drift-ambipolar (DA) heating mode
- This electric field is a combination of a drift field and an ambipolar field

Schulze et al. (2011) Phys. Rev. Lett. **107** 275001

- At 50 mTorr the electric field is zero within the electronegative core

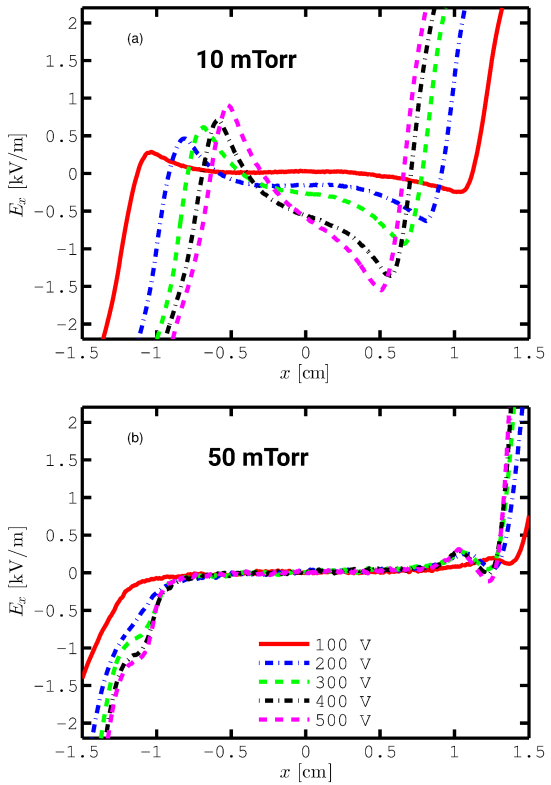


Gudmundsson and Snorrason (2017) JAP **122** 193302

# *Oxygen CCP – pressure dependence*

- The electronegativity is significantly higher when operating at 10 mTorr than when operating at 50 mTorr
- At 10 mTorr, the discharge is operated in a combined drift-ambipolar (DA) and $\alpha$-mode
- At 50 mTorr, the discharge is in a pure $\alpha$-mode and sheath heating dominates
- The transition from the combined DA-$\alpha$-mode to the pure $\alpha$-mode coincides with a significant decrease in the electronegativity

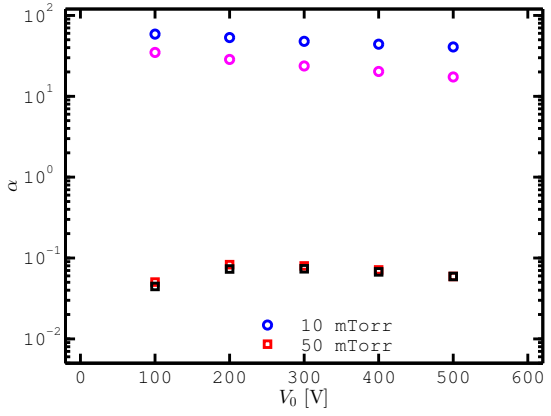


Gudmundsson and Snorrason (2017) JAP **122** 193302

# *Oxygen CCP – pressure dependence*

- At low pressure the EEPF curves outwards, the population of low energy electrons is relatively low
- As the pressure is increased the number of low energy electrons increases and the number of higher energy electrons (> 10 eV) decreases
- Thus the EEPF develops a bi-Maxwellian shape as the pressure is increased

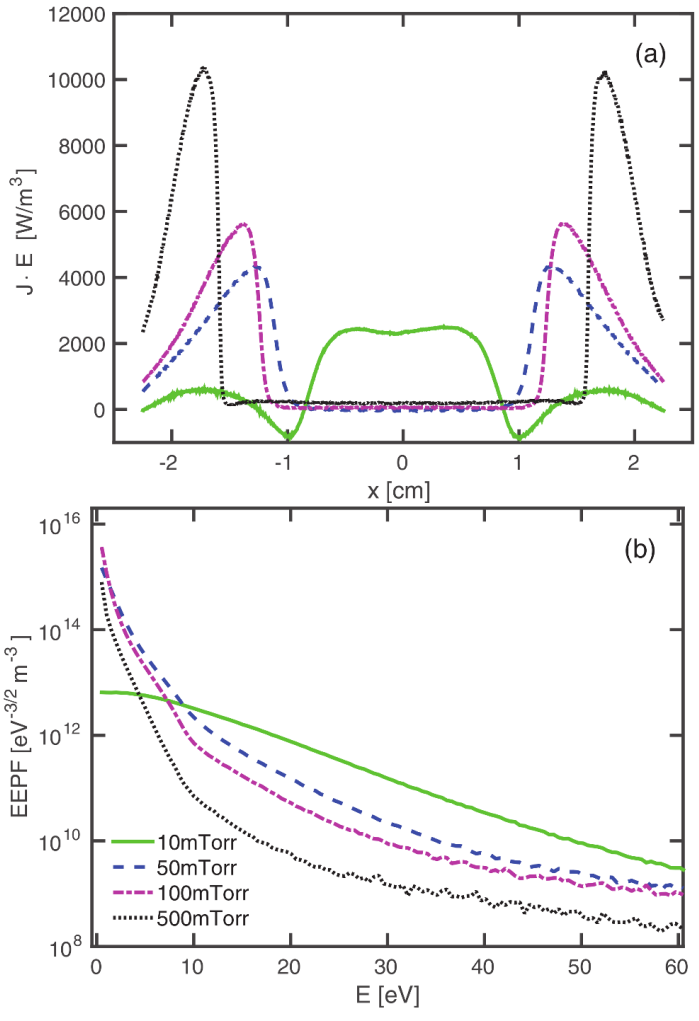



Hannesdottir and Gudmundsson (2016) PSST, **25** 055002

Gudmundsson and Ventéjou (2015) JAP **118** 153302

# Capacitively Coupled Oxygen Discharge single frequency at 10 mTorr

## – driving frequency dependence –

## including $O_2(a^1\Delta_g)$, $O_2(b^1\Sigma_g)$ and $\gamma_{see}(\mathcal{E})$

# *Oxygen CCP – frequency dependence*

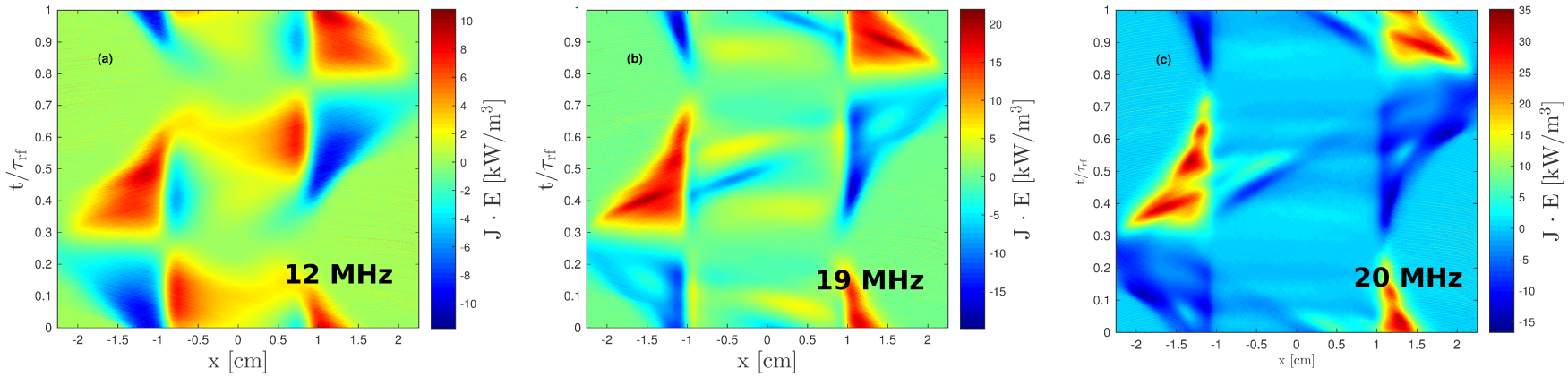


- At 12 MHz significant heating is observed in the plasma bulk but also in the sheath region
- At 19 MHz the heating and cooling in the sheath regions has increased, however there is contribution to the electron heating in the bulk region (note the change in scale)
- At 20 MHz there is almost no electron heating in the plasma bulk

# *Oxygen CCP – frequency dependence*

- At low driving frequency the EEPF is convex, the population of low energy electrons is relatively low
- The EEPF remains convex for driving frequency up to 15 MHz and has transitioned to concave or bi-Maxwellian shape at 20 MHz
- Increasing the driving frequency enhances the high energy tail as the number of high energy electrons increases

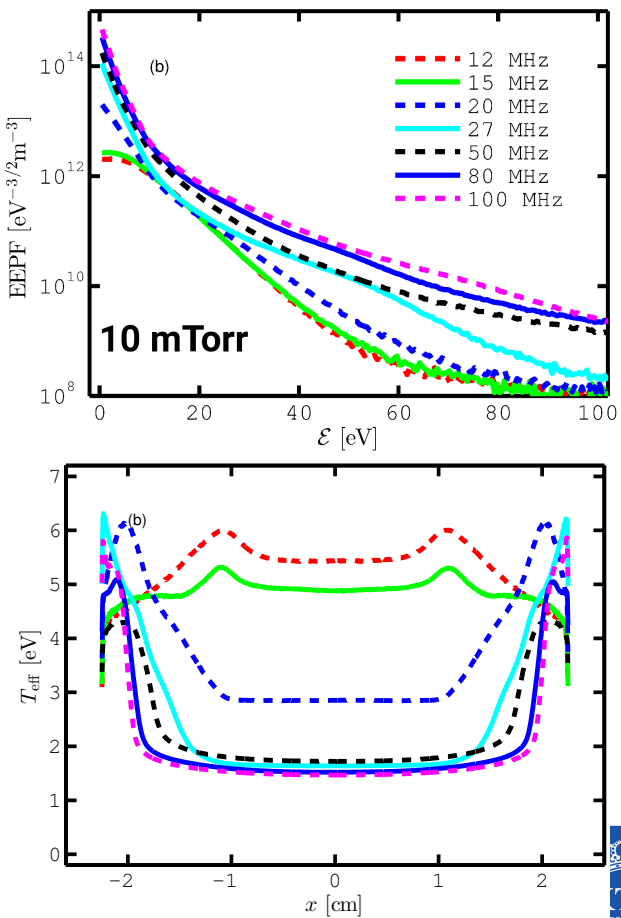


Gudmundsson et al. (2018) PSST **27** 025009

# *Oxygen CCP – frequency dependence*

- At 10 mTorr there is a jump in the center electron density between 20 and 27 MHz
- At 10 mTorr $n_e \propto f^{2.11}$ at low frequency, below 18 MHz, and $n_e \propto f^{2.00}$ at higher frequencies, 27.12 MHz and above
- At 50 mTorr $n_e \propto f^{1.16}$ over the entire frequency range explored and no transition is observed
- We see that at 5 and 10 mTorr the electronegativity decreases with increasing driving frequency

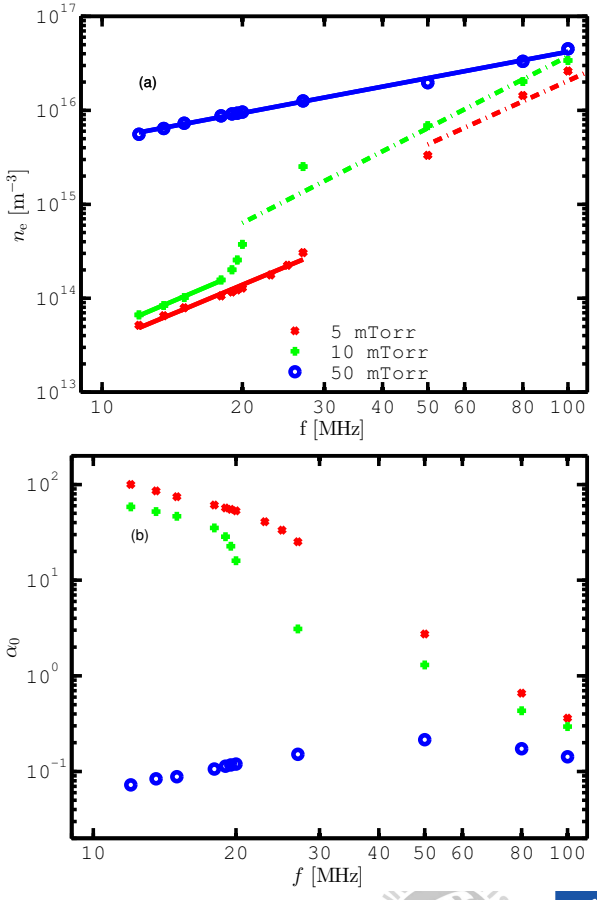


Gudmundsson et al. (2018) PSST **27** 025009

# *Oxygen CCP – frequency dependence*

- The electric field profile at $t/\tau_{\mathrm{rf}} = 0.5$ for discharges operated at 5 and 50 mTorr
- We see a significant electric field strength within the electronegative core at low driving frequency and low pressure
- The strong electric field within the plasma bulk (the electronegative core), at low pressure and low driving frequency, indicates a drift-ambipolar (DA) heating mode

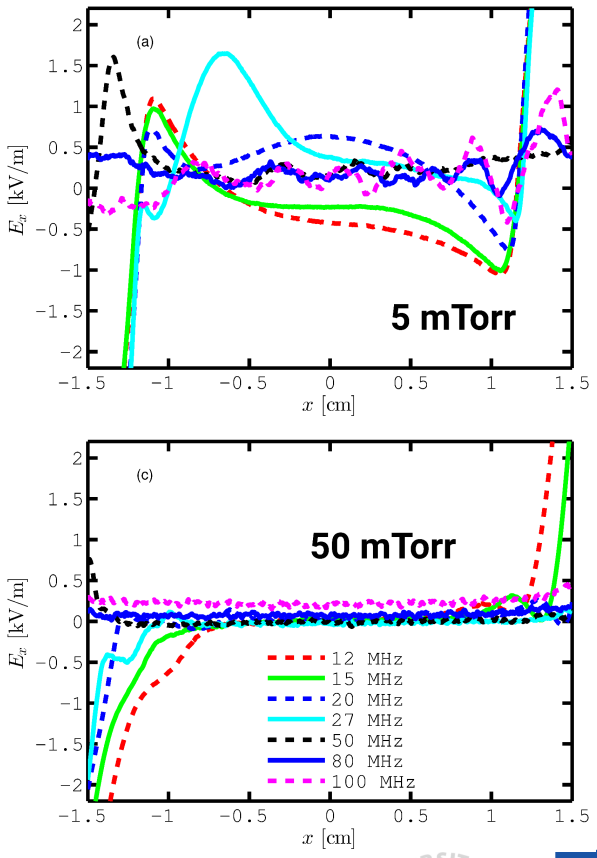


Gudmundsson et al. (2018) PSST **27** 025009

# *Oxygen CCP – frequency dependence*

- At a low driving frequency and low pressure (5 and 10 mTorr), a combination of stochastic ($\alpha$-mode) and drift ambipolar (DA) heating in the bulk plasma (the electronegative core) is observed
- The DA-mode dominates the time averaged electron heating
- As the driving frequency is increased, the heating mode transitions into a pure $\alpha$-mode
- At low pressure (5 and 10 mTorr), this transition coincides with a sharp decrease in electronegativity

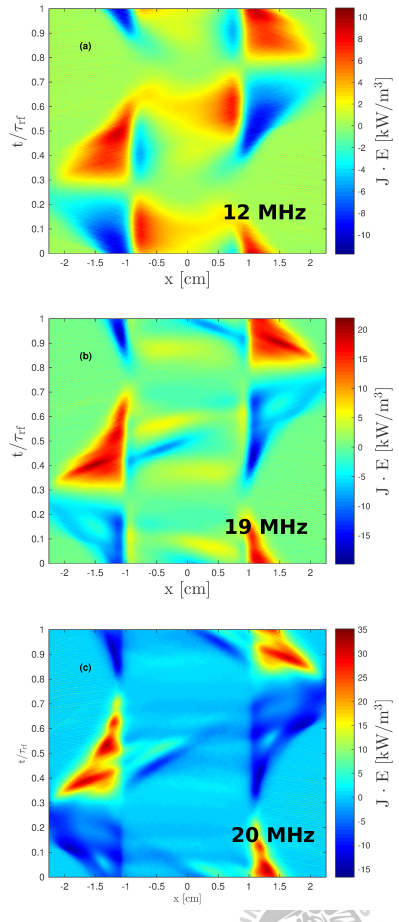


Gudmundsson et al. (2018) PSST **27** 025009

# Capacitively Coupled Oxygen Discharge

## – surface quenching of $O_2(a^1\Delta_g)$ –

## including $O_2(a^1\Delta_g)$, $O_2(b^1\Sigma_g)$ and $\gamma_{see}(\mathcal{E})$

# *Oxygen CCP – surface quenching of $O_2(a^1\Delta_g)$*

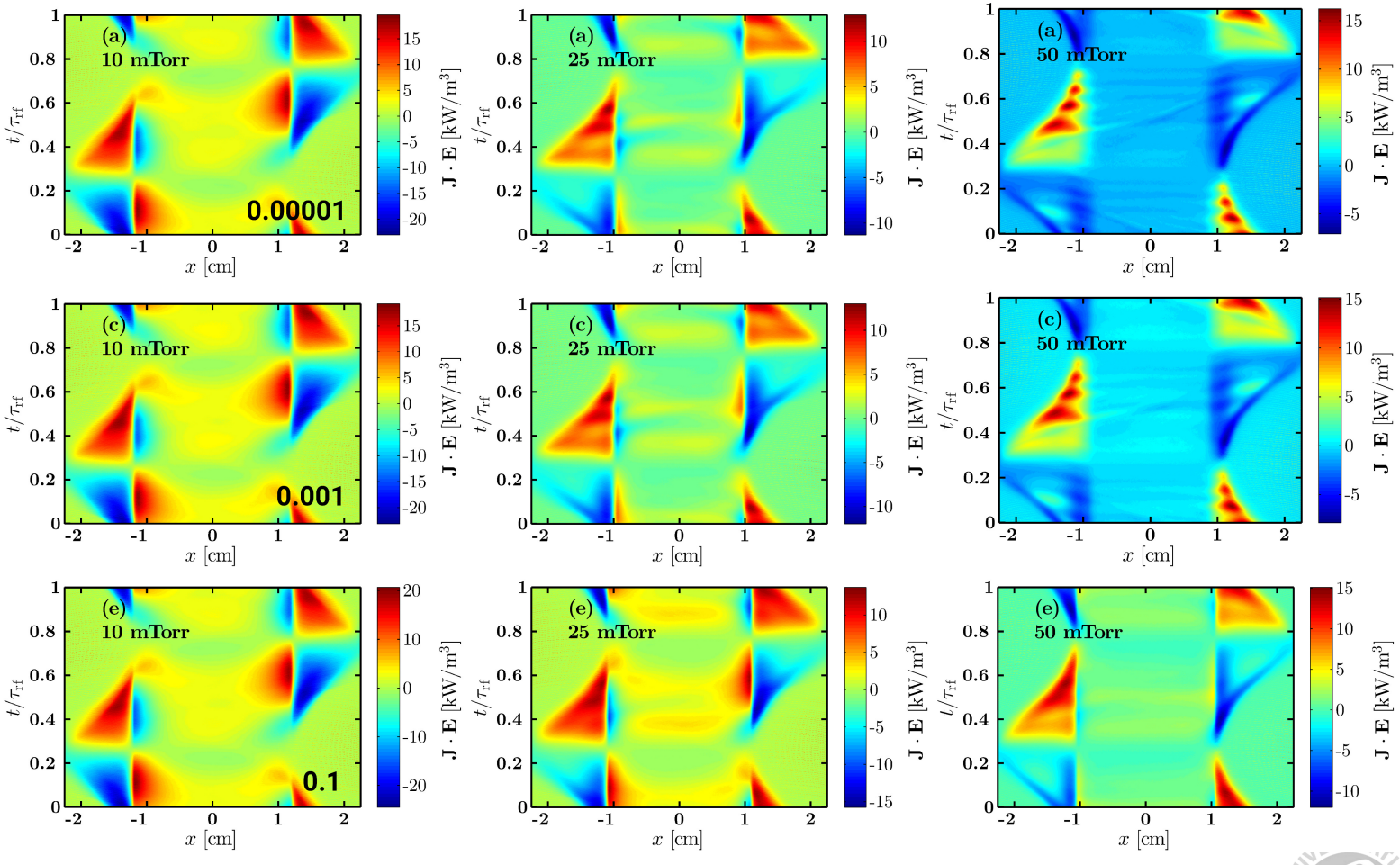


Proto and Gudmundsson (2018) PSST **27** 074002

# *Oxygen CCP – surface quenching of $O_2(a^1\Delta_g)$*

- At 10 mTorr almost all the electron heating occurs in the plasma bulk (the electronegative core) and the electron heating profile is independent of the surface quenching coefficient
- At 50 mTorr only for the highest surface quenching coefficients 0.1 and 0.01 there is some electron heating observed in the bulk region
- Typical value is 0.007 for iron (Sharpless and Slanger, 1989)

Proto and Gudmundsson (2018) PSST **27** 074002

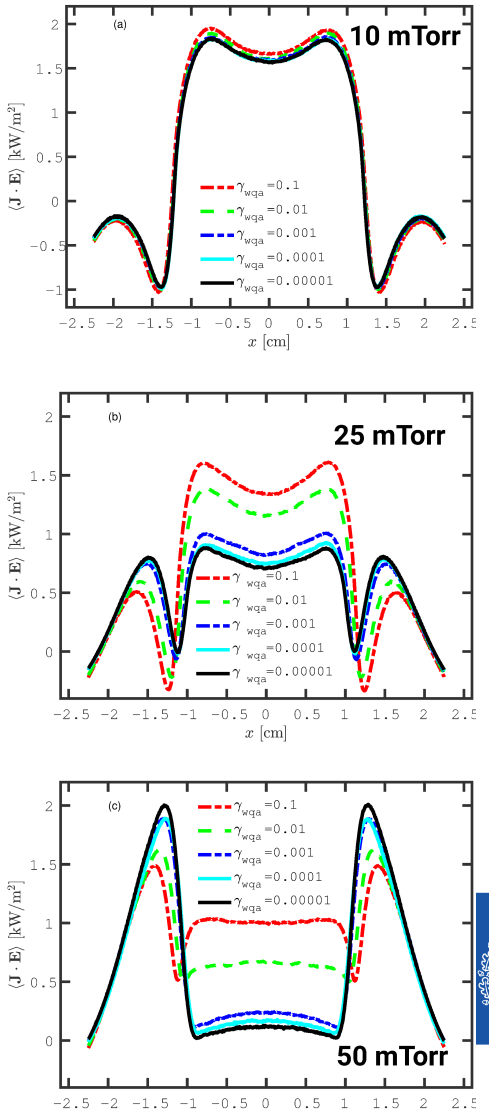

# Capacitively Coupled Oxygen Discharge

## – the effect of $\gamma_{\mathrm{see}}(\mathcal{E})$ –

## including $O_2(a^1\Delta_g)$, $O_2(b^1\Sigma_g)$ and $\gamma_{\mathrm{see}}(\mathcal{E})$

# *Oxygen CCP – the effect of* $\gamma_{\mathrm{see}}(\mathcal{E})$

- Adding secondary electron emission yield
  - increases the electron density
  - increases the electron heating rate in the sheath region
  - the sheath region becomes narrower
  - a high energy tail appears in the EEPF

Hannesdottir and Gudmundsson, PSST, **25** 055002 (2016)

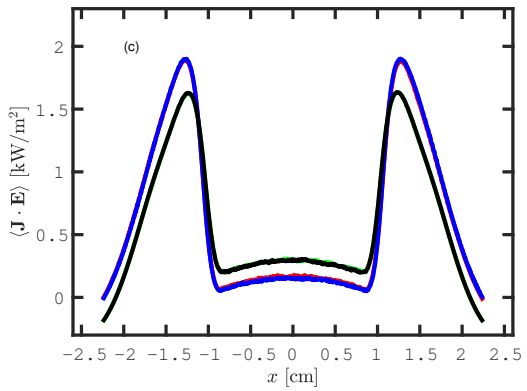


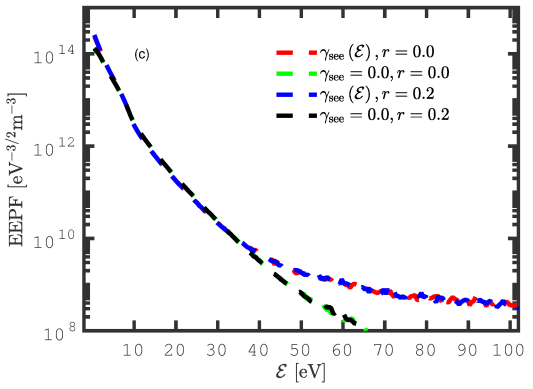

# *Oxygen CCP – the effect of* $\gamma_{\mathrm{see}}(\mathcal{E})$

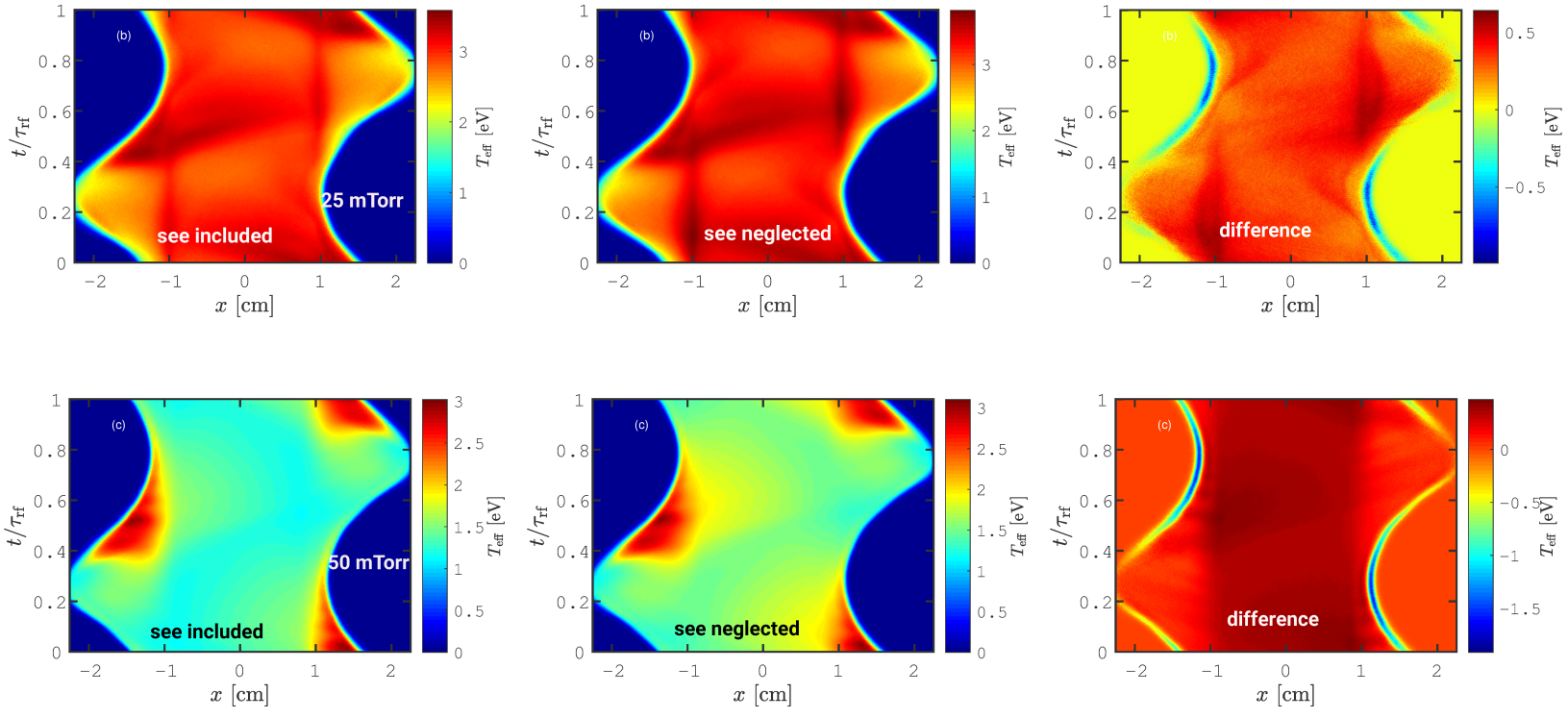


Proto and Gudmundsson (2018) Atoms (submitted September 2018)

- Including secondary electron emission increases the electron energy

# *Oxygen CCP – the effect of* $\gamma_{\mathrm{see}}(\mathcal{E})$

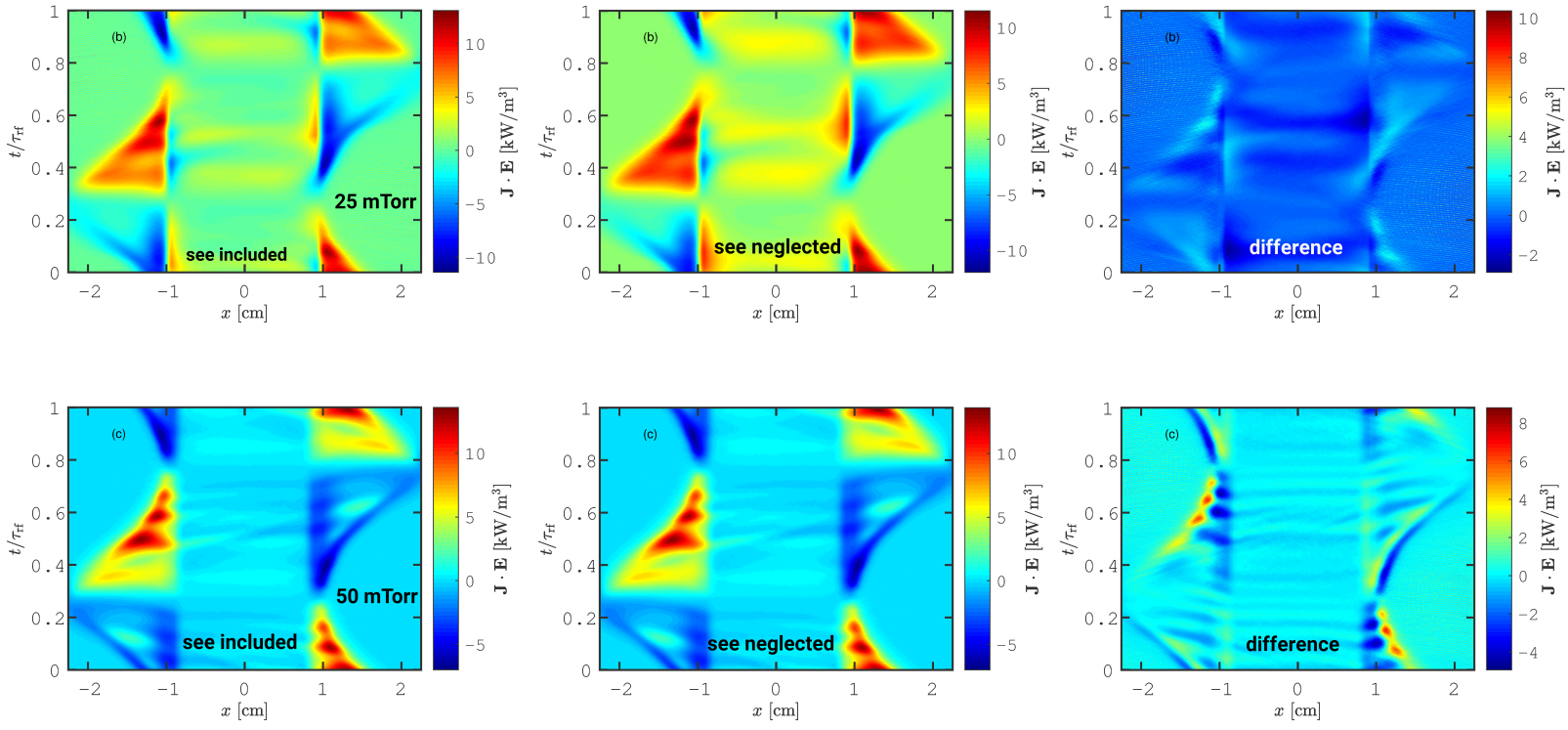


Proto and Gudmundsson (2018) Atoms (submitted September 2018)

- Including secondary electron emission decreases the electron power absorption

# Summary


SIGILLUM UNIVERSITATIS ISLANDIAE


KTH
VETENSKAP
OCH KONST

# *Summary*

- We demonstrated particle-in-cell/Monte Carlo collision simulation of a capacitively coupled discharge
- Including the detachment processes by the singlet metastable states has a strong influence on the effective electron temperature and electronegativity in the oxygen discharge
- At low pressure the discharge is operated in a combined drift-ambipolar (DA) and $\alpha$-mode, and at higher pressure it is operated in the pure $\alpha$-mode

# *Summary*

- We demonstrated particle-in-cell/Monte Carlo collision simulation of a capacitively coupled disharge
- In an oxygen discharge at low pressure the EEPF curves outward and develops a bi-Maxwellian shape as the pressure is increased
- These results contradict what is commonly found for the capacitively coupled argon discharge where the EEPF evolves from being bi-Maxwellian at low pressure to being more Druyvesteyn like at high pressure
  - the reason is the high electronegativity at low pressure in an oxygen discharge – DA heating


# C. Overall Summary


# *Overall Summary*

- A global (volume averaged) model can be used to understand the plasma chemistry
  - Which particles are important
  - Which reactions are important
  - How do the plasma parameters scale with the control parameters – power, pressure, discharge dimensions
- Particle-in-cell/Monte Carlo collision simulations can be used to explore the plasma kinetics
  - To determine the electron heating mechanism
  - To find the electron energy distribution function
  - To find the ion energy distribution (IED) and the ion angular distribution (IAD)

# *Overall Summary*

- There is clearly a need for basic experimental work on capacitively coupled oxygen discharges
  - Langmuir probe measurements, EEDF, $T_{\mathrm{eff}}$, $n_{\mathrm{e}}$ versus pressure and applied voltage
  - Electronegativity for various pressures and applied voltage
- The rate coefficient for detachment by $O_2(b^1\Sigma_g)$ has to be reevaluated
- What is the role of electron impact dissociative attachment from vibrationally excited molecular states ?
- What is the role of the metastable Herzberg states $O_2(A^3\Sigma_u^+, A'^3\Delta_u, c^1\Sigma_u^-)$ ?
- Measurements of the wall quenching coefficient of $O_2(b^1\Sigma_g)$ are needed

# *Acknowledgements*

The slides can be downloaded at
`http://langmuir.raunvis.hi.is/~tumi/ranns.html`
Various parts of this work were made by

- Eyþór Gísli Þorsteinsson (Univ. of Iceland now Men & Mice)
- Shuo Huang (UM-SJTU, Shanghai now University of Michigan)
- David A. Toneli (ITA, São José dos Campos, Brazil)
- Bruno Ventéjou (LPGP, Université Paris-Sud, Orsay, France)
- Hólmfríður Hannedóttir (University of Iceland now Harvard University)
- Davíð I. Snorrason (University of Iceland now Reykjavík University)
- Andrea Proto (University of Iceland)

in collaboration with

- prof. Michael A. Lieberman (UC Berkeley)
- prof. Allan J. Lichtenberg (UC Berkeley)
- prof. John P. Verboncoeur (Michigan State)
- Dr. Emi Kawamura (UC Berkeley)

# *References*


Godyak, V. A. (1986). *Soviet Radio Frequency Discharge Research*. Falls Church VA: Delphic Associates.

Godyak, V. A. and R. B. Piejak (1990). Abnormally low electron energy and heating-mode transition in a low-pressure argon rf discharge at 13.56 MHz. *Physical Review Letters 65*(8), 996–999.

Gudmundsson, J. T. (2001). On the effect of the electron energy distribution on the plasma parameters of argon discharge: A global (volume averaged) model study. *Plasma Sources Science and Technology 10*(1), 76–81.

Gudmundsson, J. T. and E. G. Thorsteinsson (2007). Oxygen discharges diluted with argon: dissociation processes. *Plasma Sources Science and Technology 16*(2), 399–412.

Gudmundsson, J. T. and M. A. Lieberman (2015). On the role of metastables in capacitively coupled oxygen discharges. *Plasma Sources Science and Technology 24*(3), 035016.

Gudmundsson, J. T. and D. I. Snorrason (2017). On electron heating in a low pressure capacitively coupled oxygen discharge. *Journal of Applied Physics 122*(19), 193302.

Gudmundsson, J. T., D. I. Snorrason, and H. Hannesdottir (2018). The frequency dependence of the discharge properties in a capacitively coupled oxygen discharge. *Plasma Sources Science and Technology 27*(2), 025009.

Gudmundsson, J. T., A. T. Hjartarson, and E. G. Thorsteinsson (2012). The influence of the electron energy distribution on the low pressure chlorine discharge. *Vacuum 86*(7), 808–812.

Gudmundsson, J. T., E. Kawamura, and M. A. Lieberman (2013). A benchmark study of a capacitively coupled oxygen discharge of the oopd1 particle-in-cell Monte Carlo code. *Plasma Sources Science and Technology 22*(3), 035011.

Gudmundsson, J. T. and B. Ventéjou (2015). The pressure dependence of the discharge properties in a capacitively coupled oxygen discharge. *Journal of Applied Physics 118*(15), 153302.

Guha, J., V. M. Donnelly, and Y.-K. Pu (2008). Mass and Auger electron spectroscopy studies of the interactions of atomic and molecular chlorine on a plasma reactor wall. *Journal of Applied Physics 103*(1), 013306.

Hannesdottir, H. and J. T. Gudmundsson (2016). The role of the metastable $O_2(b^1\Sigma_g^+)$ and energy-dependent secondary electron emission yields in capacitively coupled oxygen discharges. *Plasma Sources Science and Technology 25*(5), 055002.

Hjartarson, A. T., E. G. Thorsteinsson, and J. T. Gudmundsson (2010). Low pressure hydrogen discharges diluted with argon explored using a global model. *Plasma Sources Science and Technology 19*(6), 065008.

Huang, S. and J. T. Gudmundsson (2013). A particle-in-cell/Monte Carlo simulation of a capacitively coupled chlorine discharge. *Plasma Sources Science and Technology 22*(5), 055020.

# *References*


Kechkar., S. (2015, January). *Experimental investigation of a low pressure capacitively-coupled discharge*. Ph. D. thesis, Dublin City University.

Kim, S., M. A. Lieberman, A. J. Lichtenberg, and J. T. Gudmundsson (2006). Improved volume-averaged model for steady and pulsed-power electronegative discharges. *Journal of Vacuum Science and Technology A 24*(6), 2025–2040.

Lee, M.-H., H.-C. Lee, and C.-W. Chung (2010). Comparison of pressure dependence of electron energy distributions in oxygen capacitively and inductively coupled plasmas. *Physical Review E 81*(4), 046402.

Lee, C. and M. A. Lieberman (1995). Global model of Ar, $O_2$, $Cl_2$ and Ar/$O_2$ high-density plasma discharges. *Journal of Vacuum Science and Technology A 13*(2), 368–380.

Lieberman, M. A. and A. J. Lichtenberg (2005). *Principles of Plasma Discharges and Materials Processing* (2 ed.). New York: John Wiley & Sons.

Mutsukura, N., K. Kobayashi, and Y. Machi (1990). Plasma sheath thickness in radio-frequency discharges. *Journal of Applied Physics 68*(6), 2657–2660.

Proto, A. and J. T. Gudmundsson (2018). The role of surface quenching of the singlet delta molecule in a capacitively coupled oxygen discharge. *Plasma Sources Science and Technology 27*(7), 074002.

Proto, A. and J. T. Gudmundsson (2018). The influence of secondary electron emission on a capacitively coupled oxygen discharge. *Atoms* (submitted September 2018).

Schulze, J., A. Derzsi, K. Dittmann, T. Hemke, J. Meichsner, and Z. Donkó (2011). Ionization by drift and ambipolar electric fields in electronegative capacitive radio frequency plasmas. *Physical Review Letters 107*(27), 275001.

Sharpless, R. L. and T. G. Slanger (1989). Surface chemistry of metastable oxygen. II. Destruction of $O_2(a^1\Delta_g)$. *Journal of Chemical Physics 91*(12), 7947 – 7950.

Stafford, L., R. Khare, J. Guha, V. M. Donnelly, J.-S. Poirier, and J. Margot (2009). Recombination of chlorine atoms on plasma-conditioned stainless steel surfaces in the presence of adsorbed $Cl_2$. *Journal of Physics D: Applied Physics 42*(5), 055206.

Thompson, J. B. (1961). The ion balance of the oxygen d.c. glow discharge. *Proceedings of the Royal Society A 262*(1311), 519–528.

Thorsteinsson, E. G. and J. T. Gudmundsson (2010a). A global (volume averaged) model of a chlorine discharge. *Plasma Sources Science and Technology 19*(1), 015001.

# *References*


Thorsteinsson, E. G. and J. T. Gudmundsson (2010b). The low pressure $Cl_2/O_2$ discharge and the role of ClO. *Plasma Sources Science and Technology 19*(5), 055008.

Toneli, D. A., R. S. Pessoa, M. Roberto, and J. T. Gudmundsson (2015a). On the formation and annihilation of the singlet molecular metastables in an oxygen discharge. *Journal of Physics D: Applied Physics 48*(32), 325202.

Toneli, D. A., R. S. Pessoa, M. Roberto, and J. T. Gudmundsson (2015b). A volume averaged global model study of the influence of the electron energy distribution and the wall material on an oxygen discharge. *Journal of Physics D: Applied Physics 48*(49), 495203.

Vahedi, V., C. K. Birdsall, M. A. Lieberman, G. DiPeso, and T. D. Rognlien (1993). Capacitive rf discharges modelled by particle-in-cell Monte Carlo simulation. II. Comparisons with laboratory measurements of electron energy distribution functions. *Plasma Sources Science and Technology 2*(4), 273–278.

van Roosmalen, A. J., W. G. M. van den Hoek, and H. Kalter (1985). Electrical properties of planar rf discharges for dry etching. *Journal of Applied Physics 58*(2), 653–658.